Novel Natural Gas to Liquids Processes: Process Synthesis and Global Optimization Strategies

Richard C. Baliban, Josephine A. Elia, and Christodoulos A. Floudas
Dept. of Chemical and Biological Engineering, Princeton University, Princeton, NJ 08544

DOI 10.1002/aic.13996
Published online January 8, 2013 in Wiley Online Library (wileyonlinelibrary.com)

An optimization-based process synthesis framework is proposed for the conversion of natural gas to liquid transportation fuels. Natural gas conversion technologies including steam reforming, autothermal reforming, partial oxidation to methanol, and oxidative coupling to olefins are compared to determine the most economic processing pathway. Hydrocarbons are produced from Fischer–Tropsch (FT) conversion of syngas, ZSM-5 catalytic conversion of methanol, or direct natural gas conversion. Multiple FT units with different temperatures, catalyst types, and hydrocarbon effluent compositions are investigated. Gasoline, diesel, and kerosene are generated through upgrading units involving carbon-number fractionation or ZSM-5 catalytic conversion. A powerful deterministic global optimization method is introduced to solve the mixed-integer nonlinear optimization model that includes simultaneous heat, power, and water integration. Twenty-four case studies are analyzed to determine the effect of refinery capacity, liquid fuel composition, and natural gas conversion technology on the overall system cost, the process material/energy balances, and the life cycle greenhouse gas emissions. © 2013 American Institute of Chemical Engineers *AIChE J*, 59: 505–531, 2013
Keywords: process synthesis with heat, power, and water integration, GTL, Fischer–Tropsch, methanol to gasoline, methanol to olefins and distillate

Introduction

In 2010, the transportation sector consumed 13,466 thousand barrels per day (kBD) of liquid hydrocarbon fuels, representing 72.1% of the total national consumption.[1] The liquid fuel demand for transportation is expected to rise by 8% to 14,540 kBD by 2035, with the supply–demand gap being largely satisfied through "nonpetroleum" derived supply.[2] Liquid fuels that can be derived from domestic carbon-based feedstocks will ultimately reduce the dependence of crude imports from undesirable or unstable governments and can provide a significant means for increasing national security through enhanced energy independence. A recent review has highlighted the process design alternatives that can produce gasoline, diesel, and kerosene using any one or a combination of coal, biomass, or natural gas feedstocks.[3] Although multiple technologies have been proposed to process these three major feedstocks, the Energy Information Administration projects that a majority of the liquid fuels supply will come from biomass sources.[2] Corn-based ethanol and soybean-based diesel comprise a majority of the biofuels manufactured today, but their use for fuel production has led to concerns regarding the impact on the price and availability of these feedstocks as sources of food.[4] Lignocellulosic plant sources (e.g., corn stover or forest residue) could be a more considerable source of biofuels in the future, though an increase in crop production will be required to generate an appropriate amount of sustainable residue for the production of fuels.[5–7]

Liquid fuels derived from biomass or coal via a thermochemical-based route (i.e., via synthesis gas) require high investments of capital to convert the solid raw material to a clean gas product that is devoid of acidic gas species (H_2S, NH_3, and CO_2). In fact, it has been estimated that the gasification/cleanup processes needed for coal/biomass plants is approximately 50–65% of the entire plant cost.[8,9] Nevertheless, interest has continued in coal/biomass plants because of the cheap delivered cost of coal ($2.0–$2.5/MM Btu)[2] or the life cycle greenhouse gas (GHG) reduction potential of biomass.

Natural gas to liquid technologies have been studied for several decades, but were considered economically unfavorable due to the high natural gas costs. However, recent prospects for shale gas production have helped reduce the delivered cost of natural gas and made this feedstock a more attractive choice for the production of liquid fuels.[2] Natural gas is a very advantageous feedstock for the production of liquid fuels due to the high hydrogen-to-carbon ratio within a methane-rich feed. This will ultimately increase the overall yield of carbon in the liquid products, decrease the capital investment required to generate liquid products, and reduce the amount of CO_2 that is produced.

Processes using a natural gas feedstock may utilize additional carbon-based materials to combine the benefits of the different feedstocks.[3] Coal is beneficial, because the delivered cost is generally cheaper than natural gas or biomass.[2,8,10] However, the high carbon content of coal may

Additional Supporting Information may be found in the online version of this article.

Correspondence concerning this article should be addressed to C. A. Floudas at floudas@titan.princeton.edu.

require that a significant portion of the feedstock carbon be converted to CO_2 where it can either be vented, sequestered, or converted back to CO using a noncarbon-based source of hydrogen.[11–15] Biomass is highly beneficial, because it is a renewable energy source that can absorb atmospheric CO_2 during photosynthesis.[4,6,10] Examples of hybrid systems are coal and natural gas to liquids,[16–24] biomass and natural gas to liquids (BGTL),[25–28] and coal, biomass, and natural gas to liquids (CBGTL).[12–15,29,30]

Although hybrid-feedstock refineries may have significant economic or environmental benefits, it may not always be practical to utilize multiple feedstocks in an alternative energy refinery. The cost and location of a natural gas feedstock (e.g., low-value stranded natural gas) may necessitate the use of a single feedstock gas to liquids (GTL) refinery to achieve the greatest economic value for the transportation fuels. Additionally, the use of certain natural gas feedstocks that would otherwise be flared can significantly reduce the life cycle GHG emissions that are associated with the liquid products. Previous studies on GTL processes typically focus on process designs where the topology (i.e., the combination of process units and streams) is fixed. A process simulation is then conducted to determine the heat and mass balances for the process, and an economic analysis is performed to determine the viability of the plant.[16,17,20,21,28,31–47] Although a process design can be developed in this fashion, this strategy will require a significant amount of computational time and manpower to find the "best possible" design that optimizes some predetermined objective (e.g., maximum profit and minimum cost). Recent developments in process synthesis strategies for CBGTL systems[14,15,29,30] have shown that rigorous and computationally efficient methodologies exist to analyze thousands of process designs simultaneously to extract the optimal process design(s) and establish trade-offs among them. A process synthesis strategy has also been developed for switchgrass and natural gas to liquid systems[48] and a proprietary synthesis tool has been developed for GTL systems by Shell Global Solutions.[49]

This study proposes an optimization-based process synthesis framework for directly comparing the technoeconomic and environmental benefits of GTL processes in a singular mathematical model. The framework is capable of simultaneously analyzing several existing or novel processes via a process superstructure to determine the optimal topology that will have either the lowest cost or highest net present value. A rigorous global optimization strategy[29] is used to mathematically guarantee that the process design selected by the framework will have an overall cost (or profit) that is within a small percentage of the best value possible. Modeling of several components of the process superstructure has been described in detail in previous works,[14,15,29,30] though all key processes for the GTL refinery and any new components for natural gas conversion (i.e., direct conversion to methanol/olefins) will be outlined in the text later. The novelties introduced in this article include (1) the inclusion and mathematical modeling of steam reforming of natural gas, direct conversion of natural gas to methanol via partial oxidation, and direct conversion of natural gas to olefins via oxidative coupling (OC) as conversion technologies, in addition to autothermal reforming (ATR), (2) the direct usage of natural gas in the fuel combustor unit to provide process heat and in the gas turbine (GT) for electricity production, (3) different product compositions (i.e., gasoline, diesel, and kerosene) considered, namely the unrestricted composition, maximization of diesel, maximization of kerosene, and compositions commensurate with the U.S. demand ratio, and (4) calculations of the life cycle emissions of GTL systems compared with petroleum-based processes and natural gas-based electricity production. The framework includes a simultaneous heat and power integration[13,14] using an optimization-based heat-integration approach[50] and a series of heat engines that can convert waste heat into electricity.[12–14] A comprehensive wastewater treatment network[15] that utilizes a superstructure approach[51–54] to determine the appropriate topology and operating conditions of process units is utilized to minimize wastewater contaminants and freshwater intake.

The process synthesis framework will be utilized to examine (1) natural gas conversion via steam reforming, ATR, direct conversion to methanol, and direct conversion to olefins, (2) synthesis gas conversion via Fischer–Tropsch (FT) or methanol synthesis, (3) methanol conversion via methanol-to-gasoline (MTG) or methanol-to-olefins (MTO), and (4) hydrocarbon upgrading via ZSM-5 zeolite catalysis, olefin oligomerization, or boiling point fractionation and subsequent treatment. The key products from the GTL refinery will be gasoline, diesel, and jet fuel (kerosene) with allowable byproducts of liquefied petroleum gas (LPG) and electricity.

GTL Process Superstructure: Conceptual Design and Mathematical Modeling

This section will detail the modeling required to introduce additional means for natural gas conversion and the subsequent processing of the effluent streams. The complete mathematical model including all relevant nomenclature is provided as Appendix, whereas the full set of process flow diagrams (PFDs) are provided as Supporting Information.

Natural gas conditioning

Natural gas is fed to the GTL refinery at pipeline conditions of 31 bar and 25°C and is utilized in one of six major processes including ATR, steam reforming, direct coversion to methanol, direct conversion to olefins, fuel combustion, and GT electricity generation (see Figures 1 and 2). The input natural gas composition (see Table 1) is taken from the NETL Quality Guidelines for Energy Systems Studies Report and is based on the mean of over 6800 samples of pipeline quality natural gas.[55,56] Natural gas must be desulfurized to protect the catalysts in the GTL refinery, though the low sulfur concentration in pipeline natural gas ($\sim$6 ppmv[57]) will negate the need for desulfurization technology. A zinc oxide polishing bed (sulfur guard) is used to clean any mercaptan-based odorizers from the gas to prevent catalyst contamination.[56] Natural gas and other methane-rich recycle gases may be sent to a GT to produce electricity or to a fuel combustor to provide process heat (see Figure 2).[14] CO_2 produced from these units may be captured and mixed with additional process CO_2 for appropriate handling (see Figure 3).

Natural gas conversion

The natural gas leaving the sulfur guard may be converted to synthesis gas (syngas; CO, CO_2, H_2, and H_2O) via steam reforming (steam–methane-reforming [SMR]) or ATR. Both these reforming reactors will assume an equilibrium is reached for SMR (Eq. (1)) and the water–gas-shift (WGS) reaction (Eq. (2)). The effluent concentrations of C_2 and

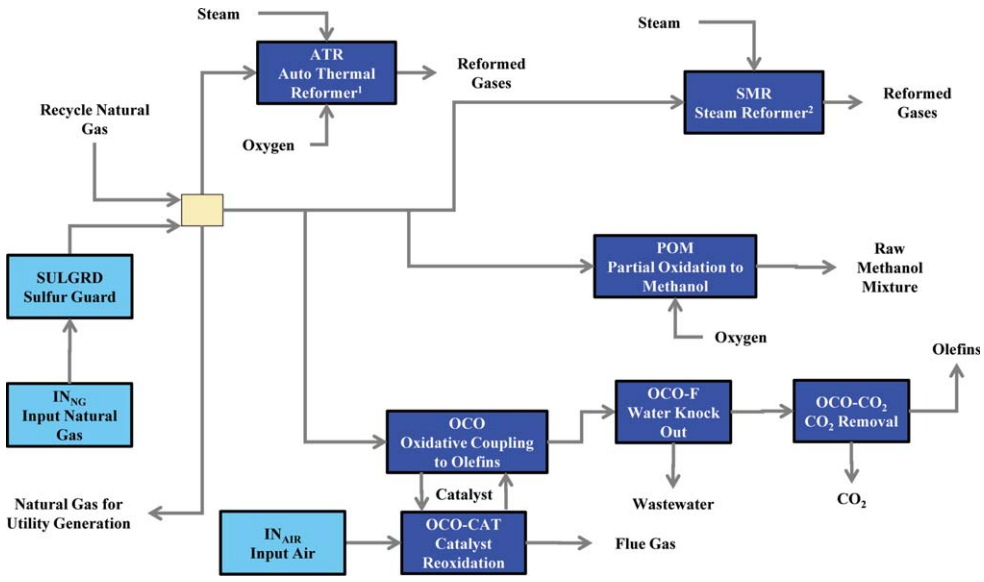

Figure 1. Natural gas conversion flow sheet.

Natural gas is combined with recycle methane and may be converted to (1) synthesis gas (CO, CO_2, H_2, and H_2O) via steam reforming or ATR, (2) methanol using catalytic partial oxidation, or (3) olefins (ethylene/propylene) via OC. [Color figure can be viewed in the online issue, which is available at wileyonlinelibrary.com.]

higher hydrocarbons are assumed to be negligible with respect to the concentration of methane.

$$CH_4 + H_2O \leftrightarrow CO + 3H_2 \quad (1)$$

$$CO_2 + H_2 \leftrightarrow CO + H_2O \quad (2)$$

Steam Reforming. Steam reforming of the natural gas uses a nickel-based catalyst contained inside high alloy steel tubes. Heat is provided for the endothermic reforming of methane via combustion of recycle fuel gas and additional input natural gas over the outside of the tubes. The reformer operates at a pressure of 30 bar with typical reaction temperatures of 700–900°C.[56] The effluent reformed gas will be constrained by both WGS equilibrium (Eq. (3)) and SMR equilibrium (Eq. (4)). The WGS equilibrium conserves the total molar flow rate, so the species molar flow rates (N^S) are sufficient to accurately define the equilibrium constraint. The SMR equilibrium constraint utilizes molar species concentrations (x^s) to account for the change in total molar flow rate. The equilibrium constant in Eq. (4) was adjusted from the value extracted from Aspen Plus for the higher pressure of the reforming unit. Although additional methods exist for defining the constraints

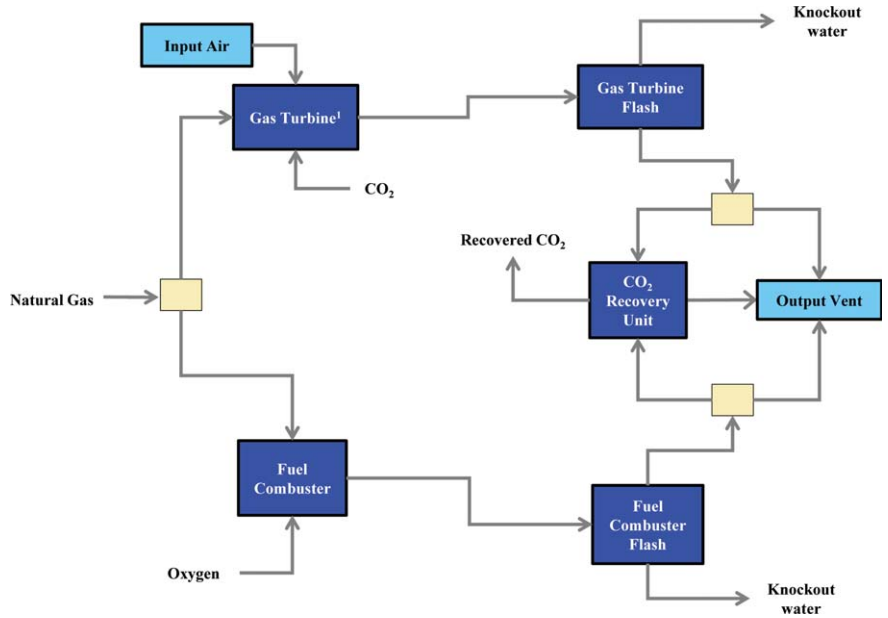

Figure 2. Flow sheet of natural gas utilities.

Natural gas and recycle fuel gas may be utilized to produce electricity through a GT or additional process heat via a fuel combustor. The effluent from both of these processes are cooled and then are either vented or passed over a CO_2 recovery unit to capture and process the produced CO_2. [Color figure can be viewed in the online issue, which is available at wileyonlinelibrary.com.]

Table 1. Molar Compositions (x) of All Species in the Input Natural Gas

Species	x
CH_4	0.931
CO_2	0.010
C_2H_6	0.032
C_3H_8	0.007
N_2	0.016
n-C_4H_{10}	0.004

in the steam reformer (e.g., molar species concentrations in WGS equilibrium), the current mathematical formulation for the steam reformer provided the best computational performance for this study. All nonhydrocarbon and nonsyngas species (e.g., N_2 and Ar) are assumed to be inert. The effluent reformed gas is directed to syngas cleaning (see Figure 3). Ambient air (13°C, 1.01 bar) is compressed to 1.1 bar to provide a 20 mol % stoichiometric excess of oxygen needed for combustion of the fuel gas within the reformer. The combusted fuel gas exits the reformer at 640°C, is cooled to 120°C to recover waste heat, and is then directed to either the stack or a CO_2 recovery unit.

$$N^{S}_{SMR,u,H_2O} \cdot N^{S}_{SMR,u,CO} = K^{WGS}_{SMR} \cdot N^{S}_{SMR,u,H_2} \cdot N^{S}_{SMR,u,CO_2} \quad (3)$$

$$x^{S}_{SMR,u,CH_4} \cdot x^{S}_{SMR,u,H_2O} = K^{MR}_{SMR} \cdot x^{S}_{SMR,u,H_2}{}^{3} \cdot x^{S}_{SMR,u,CO} \quad (4)$$

Auto-thermal Reforming. ATR of the natural gas will input a combination of steam for endothermic reforming and high-purity oxygen for partial combustion within the same reactor. The autothermal reformer will operate at a pressure of 30 bar with a temperature between 700 and 1000°C. Oxygen is provided through cryogenic air separation (99.5 wt %) or electrolysis of water (100 wt %) and is preheated to 300°C prior to entering the reformer. Steam will also be preheated to 550°C, and the natural gas will be preheated to 300°C to reduce the oxygen requirement within the reformer. The molar ratio of steam to total carbon entering the reformer will vary between 0.5 and 1.5, and the effluent will be governed by the WGS equilibrium (Eq. (5)) and SMR equilibrium (Eq. (6)). The choice of mathematical formulation of the autothermal effluent is similar to that of the steam reformer and is based on computational performance.

$$N^{S}_{ATR,u,H_2O} \cdot N^{S}_{ATR,u,CO} = K^{WGS}_{ATR} \cdot N^{S}_{ATR,u,H_2} \cdot N^{S}_{ATR,u,CO_2} \quad (5)$$

$$x^{S}_{ATR,u,CH_4} \cdot x^{S}_{ATR,u,H_2O} = K^{MR}_{ATR} \cdot x^{S}_{ATR,u,H_2}{}^{3} \cdot x^{S}_{ATR,u,CO} \quad (6)$$

The effluent from the autothermal reformer is directed to the synthesis gas cleaning section (see Figure 3).

Direct Conversion to Methanol Via Partial Oxidation. Natural gas may be directly converted to methanol via gas-phase partial oxidation operated by a free radical mechanism.[57–59] The natural gas is compressed to 52 bar and then passed into a quartz-lined tubular reactor (POM) operating at 450°C and 50 bar.[57] The per-pass conversion of methane (fc) is 13%[59] (Eq. (7)) with a carbon distribution (cd) of 63% to CH_3OH, 30% to CO, 6% to CO_2, and 1% to C_2H_6[57] (Eq. (8)), where S^{Ef}_{POM} represents the set of species that are formed from conversion of the methane. Under the reaction conditions assumed in this study, all formaldehyde is assumed to decompose quickly to H_2 and CO.[57] Oxygen is provided via an air separation unit (99.5 wt %) or electrolysis (100 wt %) with subsequent compression to 52 bar.

$$N^{S}_{POM,u,CH_4} = fc_{POM,CH_4} \cdot \sum_{(u',POM,CH_4)\in S^{UF}} N^{S}_{u',POM,CH_4} \quad (7)$$

$$N^{S}_{POM,u,s} \cdot AR_{s,C} = cd_{POM,CH_4} \cdot \sum_{(u',POM,CH_4)\in S^{UF}} N^{S}_{u',POM,CH_4} \quad \forall s \in S^{Ef}_{POM} \quad (8)$$

The effluent from the reactor is combined with the effluent from the methanol generated from synthesis gas, cooled to 35°C, and flashed to separate the methanol/water mixture.

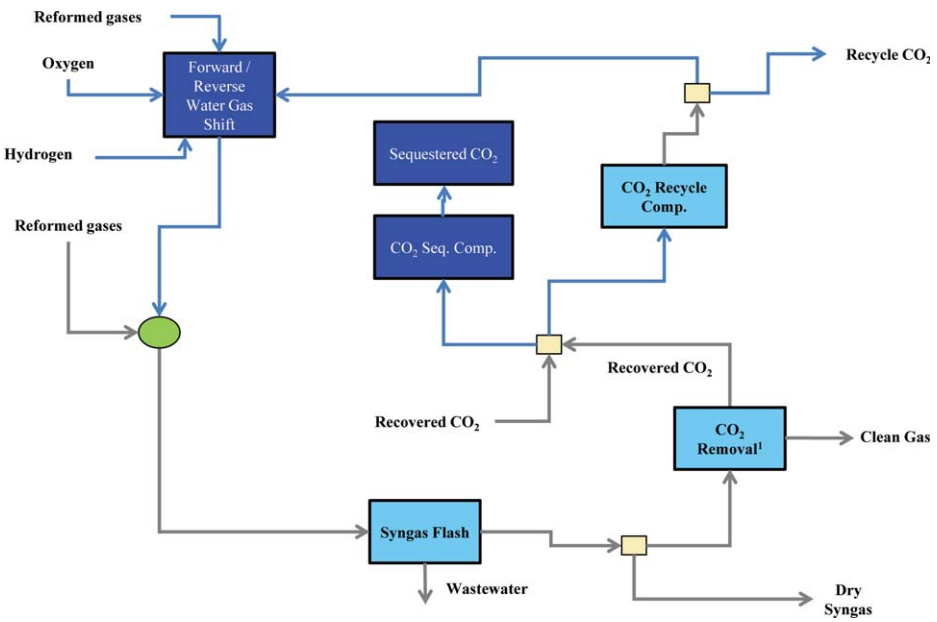

Figure 3. Synthesis gas (syngas) handling flow sheet.

Syngas may be passed over a forward/reverse WGS reactor to alter the H_2 to CO/CO_2 ratio prior to FT or methanol synthesis. The syngas is then cooled, flashed to remove water, and may be directed to a one-stage Rectisol unit for CO_2 removal. The captured CO_2 may be vented, sequestered, or recycled back to process units. [Color figure can be viewed in the online issue, which is available at wileyonlinelibrary.com.]

Table 2. Product Selectivity for OC of Natural Gas Using a 15% Mn, 5% $Na_4P_2O_y/SiO_2$ Catalyst

Temperature (°C)	800
% CH_4 conversion	25
% Selectivity of carbon	
C_2H_4	47.0
C_2H_6	14.0
C_3H_6	4.6
C_3H_8	1.4
n-C_4H_8	3.1
n-C_4H_{10}	0.9
n-C_5H_{10}	0.8
n-C_5H_{12}	0.2
Benzene	4
Toluene	0.4
CO	11
CO_2	11
Coke	1

The recycle gases are either (1) recompressed and recycled to the POM reactor, (2) heated to 500°C and expanded to 30 bar for use in a GT, or (3) heated to 500°C and expanded to 1.3 bar for use as fuel gas. The crude methanol/water mixture is combined with additional methanol from the plant prior to degassing and subsequent processing.

Direct Conversion to Olefins Via OC. Natural gas can be contacted with a reducible metal oxide catalyst to promote oxidative dehydrogenation via free radical formation.[43,60–67] The reactor (OCO) is assumed to operate at 800°C and 3.8 bar[64] with suitable expansion of the natural gas to recover electricity from a turbine. A typical CH_4 conversion (fc) over a 15% Mn, 5% $Na_4P_2O_y/SiO_2$ catalyst is 22% with a 77% selectivity (cd) to C_{2+} hydrocarbons.[61]

$$N^{S}_{OCO,u,s} = fc_{OCO,s} \cdot \sum_{(u',OCO,s)\in S^{UF}} N^{S}_{u',OCO,s} \qquad \forall s \in S^{HC}_{OCO} \quad (9)$$

$$N^{S}_{OCO,u,s} \cdot AR_{s,C} = cd_{OCO,s} \cdot \sum_{s\in S^{HC}_{OCO}} \sum_{(u',OCO,s)\in S^{UF}} N^{S}_{u',OCO,s} \qquad \forall s \in S^{Ef}_{OCO}(10) \quad (10)$$

This study will assume that the per-pass conversion of CH_4 is 25% (Eq. (9)) with a product composition shown in Table 2. The distribution of paraffins and olefins for C_2—C_5 hydrocarbons was assumed to be equal to that of the C_2 species, and the C_4—C_5 species were assumed to be linear. Equation (10) shows the mathematical constraint for distribution of carbon from the input hydrocarbons (S^{HC}_{OCO}) to all effluent species (S^{Ef}_{OCO}) in the reactor. The per-pass conversion of other light paraffins (e.g., C_nH_{2n+2}) is also assumed to be 25% with a carbon distribution to CO, CO_2, coke, and C_{n+} equivalent to that in Table 2.

The catalyst is regenerated (OCO-CAT) by passing air (10% stoichiometric excess of O_2) over the catalyst surface for reoxidation and removal of the coke to CO_2. The flue gas is cooled to 120°C to recover waste heat and is either vented or sent to a CO_2 recovery unit. The effluent of the reactor is cooled to 35°C for water knock-out (OCO—F), compressed to 50 bar, and then sent to a CO_2 removal unit (OCO—CO_2). The effluent from the CO_2 removal unit is then directed to the Mobil olefins-to-gasoline/distillate (MOGD) reactor to generate gasoline and distillate. A summary of the operating conditions within each of the four natural gas conversion units is shown in Table 3.

Synthesis gas cleaning

The PFD for processing the raw syngas from the SMR or ATR reactors is shown in Figure 3. The syngas effluent from the steam reformer or the autothermal reformer may require a forward or reverse WGS reaction depending on the reformer effluent composition and the input feed requirements for the FT or methanol synthesis. Additionally, the use of reverse WGS may provide a means for CO_2 conversion using H_2 that is either present in the input stream or recycled from the process. The WGS unit will operate at a pressure of 28 bar and a temperature between 400 and 600°C. The effluent from the WGS reactors is cooled to 35°C and sent to a water knock-out unit operating at 27.5 bar where vapor–liquid equilibrium is used to separate most of the water from the synthesis gas. The vapor effluent from the flash unit may be split to (1) a CO_2 recovery unit (e.g., one-stage Rectisol) to remove 90% of the CO_2 in the syngas or (ii) directly passed the hydrogen production/upgrading section. The clean syngas from the CO_2 recovery unit exits at 35°C and 27 bar and is sent to the hydrocarbon production/upgrading section. The CO_2 from the Rectisol unit exits at 1.5 bar and 49°C and may be (a) compressed to 31 bar for recycle to the reformers or the WGS units or (b) compressed to 150 bar for sequestration. Note that both compression options will utilize multiple compression stages with intercooling to control the temperature rise. The CO_2 may alternatively be vented to the atmosphere.

Hydrocarbon production/upgrading

FT Hydrocarbon Production. The hydrocarbon production section (Supporting Information, Figures S4 and S7) will convert the syngas using either FT synthesis or methanol synthesis. The FT units will operate at 20 bar and will utilize either a cobalt-based or iron-based catalyst.[14,15,30] The cobalt-based units will require a CO_2-lean synthesis gas feed to prevent poisoning of the FT catalyst and increase conversion of the CO. The iron-based catalysts may use either the CO_2-lean or CO_2-rich syngas, because the WGS reaction will be facilitated by the iron catalyst. Therefore, these reactors could consume CO_2 within the unit using H_2 to produce the CO necessary for the FT reaction.[14,15,30]

Synthesis gas is split to either the low-wax FT section (SP_{FTM}), the nominal-wax FT section (SP_{FTN}), or methanol synthesis (MEOHS). The FT units will operate within the temperature range of 240–320°C. The cobalt-based FT units operate at either low temperature (LTFT; 240°C) or high temperature (HTFT; 320°C) and must have a minimal amount of CO_2 in the input stream. Two iron-based FT units will facilitate the WGS reaction and will operate at low (LTFTRGS; 240°C) and high temperature (HTFTRGS; 320°C). The other two iron-based FT units will operate at a mid-level temperature (267°C), and produce either minimal (MTFTWGS-M) or nominal (MTFTWGS-N) amounts of wax. Each of the four iron-based FT units may facilitate either the forward or the reverse WGS reaction.

Table 3. Operating Conditions for the Direct or Indirect Conversion of Natural Gas

Unit	Temperature (°C)	Pressure (bar)	Conv. of CH_4(%)
Autothermal reformer	700–1000	30	80–95
Steam reformer	700–900	30	80–95
Partial oxidation	450	50	13
OC	800	3.8	25

Hydrogen may be recycled to any of the FT units to either shift the H_2/CO ratio or the H_2/CO_2 ratio to the appropriate level. Steam may alternatively be used as a feed for the two iron-based fWGS FT units to shift the H_2/CO ratio. CO_2 may be recycled back to the iron-based FT units to be consumed in the WGS reaction. Similarly, the pressure-swing adsorption (PSA) offgas, which will be lean in H_2, may be recycled to the iron-based FT units for consumption of the CO or CO_2. The effluent from the autothermal reactor (ATR) will contain a H_2/CO ratio that is generally above 2/1 and is, therefore, favorable as a feedstock for FT synthesis.[10] However, the concentration of CO_2 within the ATR effluent will prevent the stream from being fed to the cobalt-based units. The two streams exiting the FT units will be a waxy liquid phase and a vapor phase containing a range of hydrocarbons. The wax will be directed to a hydrocracker (WHC), whereas the vapor phase is split (SP_{FTH}) for further processing.

FT Hydrocarbon Upgrading. The vapor phase effluent from FT synthesis will contain a mixture of C_1—C_{30+} hydrocarbons, water, and some oxygenated species. Supporting Information, Figure S5 details the process flow sheet used to process this effluent stream. The stream will be split and can pass through a series of treatment units designed to cool the stream and knock out the water and oxygenates for treatment. Initially, the water-soluble oxygenates are stripped from the stream. The stream is then passed to a three-phase separator to remove the aqueous phase from the residual vapor and any hydrocarbon liquid. Any oxygenates that are present in the vapor phase may be removed using an additional separation unit. The water lean FT hydrocarbons are then sent to a hydrocarbon recovery column for fractionation and further processing (Supporting Information, Figure S6). The oxygenates and water removed from the stream are mixed and sent to the biological digestor for wastewater treatment.

The FT hydrocarbons may also be passed over a ZSM-5 catalytic reactor operating at 408°C and 16 bar[68] to be converted into mostly gasoline range hydrocarbons and some distillate.[68,69] The ZSM-5 unit will be able to convert the oxygenates to additional hydrocarbons, so no separate processing of the oxygenates will be required for the aqueous effluent. The raw product from FT-ZSM5 is fractionated to separate the water and distillate from the gasoline product. The water is mixed with other wastewater knock-out, and the distillate is hydrotreated to form a diesel product. The raw ZSM-5 HC product is sent to the LPG–gasoline separation section for further processing (Supporting Information, Figure S8).

The water lean FT hydrocarbons are sent to a hydrocarbon recovery column, as shown in Supporting Information, Figure S6. The hydrocarbons are split into C_3—C_5 gases, naphtha, kerosene, distillate, wax, offgas, and wastewater.[12,70] The upgrading of each stream will follow a detailed Bechtel design,[70,71] which includes a wax hydrocracker, a distillate hydrotreater, a kerosene hydrotreater, a naphtha hydrotreater, a naphtha reformer, a C_4 isomerizer, a C_5/C_6 isomerizer, a $C_3/C_4/C_5$ alkylation unit, and a saturated gas plant.

Methanol Synthesis. The methanol synthesis reactor (Supporting Information, Figure S7) will operate at 300°C and 50 bar and may input either the CO_2-rich or CO_2-lean syngas. The syngas leaving the cleaning section must be compressed to 51 bar prior to entering the methanol synthesis reactor. The methanol synthesis reactor will assume equilibrium is achieved for the WGS reaction (Eq. (12)) and the methanol synthesis reaction (Eq. (11)).

$$CO + 2H_2 \leftrightarrow CH_3OH \quad (11)$$

$$CO_2 + H_2 \leftrightarrow CO + H_2O \quad (12)$$

The typical per-pass conversion of CO and CO_2 to methanol is ~35%,[72] and the relative concentration of H_2O to methanol in the effluent stream is largely determined based on the input concentration of CO_2 to the reactor. The effluent from the reactor is cooled to 35°C, and a crude methanol stream is separated using vapor–liquid equilibrium at 48 bar. The amount of methanol that is entrained in the vapor phase is dependent on the input concentration of syngas to the flash unit, but a majority (over 95%) of the methanol can be recovered by enforcing a stoichiometric amount of H_2 in the input to the synthesis reactor (i.e., $H_2/(2CO + 3CO_2) = 1$). The vapor stream from the flash unit is split, so that 5% may be purged to remove inert species, and the remaining 95% is compressed to 51 bar and then recycled to the methanol synthesis reactor. The purge stream is recycled back to the process and used as fuel gas.

The crude methanol product from the flash unit is heated to 200°C, expanded to 5 bar to recover electricity, and then cooled to 60°C prior to entering a degasser distillation column. The degasser will remove all the entrained gases from the liquid methanol/water while recovering 99.9% of the methanol. The entrained gases are recycled back to the process for use as fuel gas. The bottoms from the degasser will contain methanol and water, with a methanol composition dependent on the level of CO_2 input to the synthesis unit. High levels of water in the liquid stream are not anticipated to be a concern, because the downstream methanol processing units will yield 50 wt % water from the hydrocarbon synthesis.

Methanol Conversion. The purified methanol is split to either the MTG process or to the MTO and MOGD processes. The MTG process will catalytically convert the MTG range hydrocarbons using a ZSM-5 zeolite and a fluidized bed reactor. The MTG effluent is outlined in Table 3.4.2 of the Mobil study[73] and in PFD P850-A1402 of the NREL study.[72] Due to the high level of component detail provided by NREL for both the MTG unit and the subsequent gasoline product separation units, the composition of the MTG reactor used in this study is based on the NREL report. The MTG unit will operate adiabatically at a temperature of 400°C and 12.8 bar. The methanol feed will be pumped to 14.5 bar and heated to 330°C for input to the reactor. The methanol will be converted to 44 wt % water and 56 wt % crude hydrocarbons, of which 2 wt % will be light gas, 19 wt % will be C_3—C_4 gases, and 19 wt % will be C_{5+} gasoline.[72] The crude hydrocarbons will ultimately be separated into finished fuel products, of which 82 wt % will be gasoline, 10 wt % will be LPG, and the balance will be recycle gases. This is modeled mathematically in the process synthesis model using an atom balance around the MTG unit and assuming a 100% conversion of the methanol entering the MTG reactor.[72,73]

Any methanol entering the MTO process unit is heated to 400°C at 1.2 bar. The MTO fluidized bed reactor operates at a temperature of 482°C and a pressure of 1 bar. The exothermic heat of reaction within the MTO unit is controlled through generation of low-pressure steam. One hundred

percent of the input methanol is converted into olefin effluent containing 1.4 wt % CH_4, 6.5 wt % C_2—C_4 paraffins, 56.4 wt % C_2—C_4 olefins, and 35.7 wt % C_5—C_{11} gasoline.[74] The MTO unit is modeled mathematically using an atom balance and a typical composition seen in the literature.[74] The MTO product is fractionated (MTO-F) to separate the light gases, olefins, and gasoline fractions. The MTO-F unit is assumed to operate as a separator unit where 100% of the C_1—C_3 paraffins are recycled back to the refinery, 100% of the C_4 paraffins and 100% of the olefins are directed to the MOGD unit, 100% of the gasoline is combined with the remainder of the gasoline generated in the process, and 100% of the water generated in the MTO unit is sent for wastewater treatment.

The separated olefins are sent to the MOGD unit where a fixed bed reactor is used to convert the olefins to gasoline and distillate over a ZSM-5 catalyst. The gasoline/distillate product ratios can range from 0.12 to >100, and the ratio chosen in this study was 0.12 to maximize the production of diesel. The MOGD unit operates at 400°C and 1 bar and will utilize steam generation to remove the exothermic heat of reaction within the unit. The MOGD unit is modeled with an atom balance and will produce 82% distillate, 15% gasoline, and 3% light gases.[74] The product will be fractionated (MTODF) to remove diesel and kerosene cuts from the gasoline and light gases. The MTODF unit will be modeled as a separator unit where 100% of the C_{11}—C_{13} species are directed to the kerosene cut and 100% of the C_{14+} species are directed to the diesel cut.

LPG–Gasoline Separation. The LPG and gasoline generated from ZSM-5 conversion of the FT hydrocarbons or the methanol must be passed through a series of separation units to extract the LPG from the gasoline and alkylate any isobutane to a blending stock for the final gasoline pool (Supporting Information, Figure S8). Light gases are initially removed via one of two knock-out units, and the crude hydrocarbons are passed through a de-ethanizer column, a stabilizer column, an absorber column, a splitter column, and an LPG alkylate splitter to separate the LPG from the gasoline fractions. Each of these units is modeled mathematically as a splitter unit where the split fraction of each species to an output stream is given by the information in the PFDs P850-A1501 and P850-A1502 from the NREL study.[72] All low-pressure steam and cooling water needed for each of the units is derived for each of the units in the NREL study. The total amount of process utility that is needed per unit flow rate from the top or bottom of the column is calculated, and this ratio is used as a parameter in the process synthesis model to determine the actual amount of each utility needed based on the unit flow rate.

In addition to the distillation columns within this section, there is also an alkylation unit that is used to convert isobutane and butene to an alkylate blending stock for the gasoline pool. The alkylate was modeled as isobutane,[72] and the alkylation unit was modeled using a species balance where the key species, butene, was completely converted to isobutane. Butene is used as the limiting species in this reaction, because it is generally present in a far smaller concentration than isobutane.

Hydrogen/oxygen production

Hydrogen is produced via pressure-swing adsorption or an electrolyzer unit, whereas oxygen can be provided by the electrolyzer or a separate air separation unit (Supporting Information, Figure S9).

Wastewater treatment

A complete wastewater treatment network (Supporting Information, Figures S10 and S11) is incorporated that will treat and recycle wastewater from various process units, blowdown from the cooling tower, blowdown from the boilers, and input freshwater.[15] Process wastewater is treated using only a biological digestor due to the negligible quantities of sulfur (e.g., H_2S) or nitrogen (e.g., NH_3) that are expected to be in the wastewater streams. Clean output of the network includes (1) process water to the electrolyzers, (2) steam to the autothermal reformer, steam reformer, and WGS reactor, and (3) discharged wastewater to the environment.

Unit costs

The total direct costs, TDC, for the GTL refinery hydrocarbon production and upgrading units are calculated using estimates from several literature sources[68,69,72,73,75] using the cost parameters in Table 4 and Eq. 13

$$\mathrm{TDC} = (1 + \mathrm{BOP}) \cdot C_o \cdot \frac{S_r^{\,sf}}{S_o} \tag{13}$$

where C_o is the installed unit cost, S_o is the base capacity, S_r is the actual capacity, sf is the cost scaling factor, and BOP is the balance of plant percentage (site preparation, utility plants, etc.). The BOP is estimated to be 20% of the total installed unit cost. All capital cost numbers are converted to 2011 dollars using the Chemical Engineering Plant Cost Index.[76] The cost estimates for the four natural gas conversion technologies are included in Table 4. Cost estimates for all other process units in the GTL refinery are taken from previous works and are included in the Supporting Information.[14,15,30]

The total plant cost, TPC, for each unit is calculated as the sum of the total direct capital, TDC, plus the indirect costs, IC. The IC include engineering, startup, spares, royalties, and contingencies and is estimated to 32% of the TDC. The TPC for each unit must be converted to a levelized cost to compare with the variable feedstock and operational costs for the process. Using the methodology of Kreutz et al.,[8] the capital charges (CC) for the refinery are calculated by multiplying the levelized capital charge rate (LCCR) and the interest during construction factor (IDCF) by the total overnight capital (Eq. (14)).

$$\mathrm{CC} = \mathrm{LCCR} \times \mathrm{IDCF} \times \mathrm{TPC} \tag{14}$$

Kreutz et al.[8] calculates an LCCR value of 14.38%/yr and and IDCF of 7.6%. Thus, a multiplier of 15.41%/yr is used to convert the TPC into a capital charge rate. Assuming an operating capacity (CAP) of 330 days/yr and operation/maintenance (OM) costs equal to 5% of the TPC, the total levelized cost (Cost^U) associated with a unit is given by Eq. (15).

$$\mathrm{Cost}_u^U = \left(\frac{\mathrm{LCCR} \times \mathrm{IDCF}}{\mathrm{CAP}} + \frac{\mathrm{OM}}{365}\right) \cdot \left(\frac{\mathrm{TOC}_u}{\mathrm{Prod}}\right) \tag{15}$$

The levelized costs for the units described for natural gas conversion are added to the complete list of GTL process units in previous studies.[14,15,29,30]

Objective function

The objective function for the model is given by Eq. (16). The summation represents the total cost of liquid fuels production and includes contributions from the feedstocks cost

Table 4. GTL Refinery Wastewater Treatment Reference Capacities, Costs (2011$), and Scaling Factors

Description	C_o (MM $)	S_o	S_{Max}	Units	Scale Basis	sf	Ref.
Autothermal reformer	10.26	12.2	35.0	kg/s	Natural gas feed	0.67	71
Steam–methane reformer	63.74	26.1	35.0	kg/s	Natural gas feed	0.67	57
Partial oxidation reactor	650.1	118.8	75.0	kg/s	Natural gas feed	0.67	65
OC reactor	287.62	661.9	75.0	kg/s	Natural gas feed	0.67	65

for natural gas ($Cost^F_{NG}$), freshwater ($Cost^F_{H_2O}$), and butanes ($Cost^F_{BUT}$), the electricity cost ($Cost^{El}$), the CO_2 transportation, storage, and monitoring cost ($Cost^{Seq}$), and the levelized unit investment cost ($Cost^U$). Each of the terms in Eq. (16) is normalized to the total volume of products produced (Prod). Note that other normalization factors (e.g., total volume of gasoline equivalent and total energy of products) and other objective functions (e.g., maximizing the net present value) can be easily incorporated into the model framework.

$$\text{MIN}\ Cost^F_{NG} + Cost^F_{H_2O} + Cost^F_{BUT} + Cost^{El} + Cost^{Seq} + \sum_{u \in U_{Inv}} Cost^U_u \tag{16}$$

The process synthesis model with simultaneous heat, power, and water integration represents a large-scale nonconvex mixed-integer nonlinear optimization model that was solved to global optimality using a branch-and-bound global optimization framework.[29] At each node in the branch-and-bound tree, a mixed-integer linear relaxation of the mathematical model is solved using CPLEX,[77] and then, the node is branched to create two children nodes. The solution pool feature of CPLEX is utilized during the solution of the relaxed model to generate a set of distinct points (150 for the root node and 10 for all other nodes), each of which is used as a candidate starting point to solve the original model. For each starting point, the current binary variable values are fixed, and the resulting NLP is minimized using CONOPT.[78] If the solution to the NLP is less than the current upper bound, then the upper bound is replaced with the NLP solution value. At each step, all nodes that have a lower bound that is within an ϵ tolerance of the current upper bound $\left(\frac{LB_{node}}{UB} \geqslant 1-\varepsilon\right)$ are eliminated from the tree. For a more complete coverage of branch-and-bound algorithms, the reader is directed to the textbooks of Floudas[79,80] and reviews of global optimization methods.[81–83]

Computational Studies

The process synthesis model (see Appendix and Supporting Information) was used to analyze 24 distinct case studies using an average representation of natural gas feedstock (Table 1). The global optimization framework was terminated, if all nodes in the branch-and-bound tree were processed or if 100 CPU hours had passed.[29] The case studies were chosen to examine the effect of (1) plant capacity, (2) product composition, (3) natural gas conversion technology, and (4) GHG reduction requirement on the overall cost of fuel production and the optimal process topology. Four representative capacities of 1, 10, 50, and 200 kBD were chosen to examine the potential effect of economy of scale. The capacity of the plants is defined as "barrels per stream day," which is computed by dividing the total number of produced barrels by the actual number of days that the GTL refinery was operational. All of the units are, therefore, appropriately sized to a "barrels per calendar day" figure using the capacity factor of the refinery (Eq. (15)). Liquid fuel (i.e., gasoline, diesel, and kerosene) production was selected to either (a) represent the 2010 United States demand (i.e., 67 vol % gasoline, 22 vol % diesel, and 11 vol % kerosene),[84] (b) maximize the diesel production (i.e., $\geqslant$75 vol %), (c) maximize the kerosene production (i.e., $\geqslant$70 vol %), or (d) freely output any unrestricted composition of the products. These case studies will be labeled as $N - C$, where N represents the type of product composition (i.e., R: 2010 U.S. ratios, D: max diesel, K: max kerosene, and U: unrestricted composition) and C represents the capacity in kBD. For example, the U-1 label represents the 1 kBD capacity refinery with an unrestricted product composition.

A second set of case studies will examine the effects of the natural gas conversion technology on the U-1 refinery. In each case study, the natural gas conversion technology will be fixed to either ATR, steam reforming, partial oxidation to methanol, or OC to olefins. These studies will be labeled as *G*-U-1, where *G* represents the type of natural gas conversion technology (i.e., A: ATR, S: steam reforming, P: partial oxidation, and C: OC). Each of the 20 case studies described earlier will ensure that the life cycle GHG emissions from the refinery are at most equal to current fossil-fuel-based processes. That is, the life cycle GHG emissions must be at most equal to that of a petroleum-based refinery (91.6 kg CO^{2eq}/GJ^{LHV}) for the liquid fuels or that of a natural gas combined cycle plant (101.3 kg CO^{2eq}/GJ) for electricity. The final four case studies will examine the effect of the utilization of CO_2 capture and sequestration on all vented streams from the refineries with an unrestricted product composition. For each of the four refinery capacities, a maximum of 1% of the input carbon will be allowed to be vented to the atmosphere as CO_2. The balance of the carbon must be contained within the liquid fuels or in CO_2 that is compressed and then sequestered. For each capacity, C, the case study will be labeled as U-*C*-Z.

The cost parameters[14,15] used for the GTL refinery are listed in Table 5. The costs for feedstocks (i.e., natural gas, freshwater, and butanes) include all costs associated with delivery to the plant gate. The products (i.e., electricity and propane) are assumed to be sold from the plant gate and do not include the costs expected for transport to the end consumer. The cost of CO_2 capture and compression is included in the investment cost of the GTL refinery, whereas the cost for transportation, storage, and monitoring of the CO_2 is shown in Table 5.

Once the global optimization algorithm has completed, the resulting process topology provides (1) the operating conditions and working fluid flow rates of the heat engines, (2) the amount of electricity produced by the heat engines, (3) the amount of cooling water needed for the engines, and (4) the location of the pinch points denoting the distinct subnetworks. Given this information, the minimum number of heat exchanger matches necessary to meet specifications (1)–(4) are calculated as previously described.[14,15,79,85] On solution of the minimum matches model, the heat exchanger topology with the minimum annualized cost can be found using the superstructure methodology.[13,79,85] The investment cost of

Table 5. Cost Parameters (2011$) for the CBGTL Refinery

Item	Cost	Item	Cost
Natural gas	$5/TSCF[a]	Freshwater	$0.50/metric ton
Butanes	$1.84/gallon	Propanes	$1.78/gallon
Electricity	$0.07/kW h	CO_2 TS&M[b]	$5/metric ton

[a]TSCF—thousand standard cubic feet.
[b]TS&M—transportation, shipping, and monitoring.

the heat exchangers is added to the investment cost calculated within the process synthesis model to obtain the final investment cost for the superstructure.

Optimal process topologies

Key information about the optimal process topologies for all case studies is shown in Table 6. For natural gas conversion (NG conv.), the possible choices are steam reforming (SMR), ATR, partial oxidation to methanol (PO), and OC. Three possible temperature options were used for the steam reformer (700, 800, and 900°C), the autothermal reformer (800, 900, and 1000°C), and the reverse WGS unit (400, 500, and 600°C). For the 20 case studies that did not constrain the natural gas conversion technology, either the steam reformer or the autothermal reformer was selected as the optimal unit. Additionally, the operating temperatures of these units were consistently chosen to be at the upper operating limit (900°C for SMR and 1000°C for ATR). The choice of operating temperature within the reformers represents a balance among (1) the level of input steam needed, (2) the extent of consumption of CO_2 via the reverse WGS reaction, (3) the extent of methane conversion, and (4) the fuel gas or oxygen requirement to provide process heating. Lower reformer temperatures will have less favorable conditions for methane conversion and CO_2 consumption due to lower values of the equilibrium constants in the reformer. Alternatively, both the steam and the heating requirement will be smaller, decreasing the operating costs of the unit. Higher temperatures will have higher conversions of methane and CO_2 with a correspondingly higher steam and heating requirement. Selection of the high-temperature units shows that a key topological decision is the conversion of methane and CO_2 in the reformers. The decrease in the capital requirement of the downstream process units outweights the increased operating costs with a higher temperature.

Selection of a specific reformer to convert the natural gas is critical for two major reasons. First, though the cost of a steam reformer is higher than the autothermal reformer (see Table 4), the additional cost of air separation to produce high-purity oxygen makes the autothermal reformer a more capital intensive choice to produce synthesis gas at lower capacity levels. However, as the refinery capacity increases, there is a definable point where the capital and operating costs of steam reforming are greater than the sum of ATR and air separation. A key insight can be found by observing that the scaling factor of the reforming units is assumed to by 0.67 (Table 4), whereas that of the air separation unit is assumed to be 0.5 based on the study by Kreutz et al.[8] (see Supporting Information, Table S1). At some critical capacity level, the capital cost of the air separation unit and the autothermal reformer will be equal to that of a steam reformer, and it is anticipated that higher capacity levels will favor ATR, whereas lower capacity levels favor steam reforming. This is evident when comparing case studies A-U-1 and S-U-1. Table 8 shows that the use of an autothermal reformer adds about 5% to the investment cost of the plant and ultimately increases the cost of liquid fuels by 7%.

Second, the use of an autothermal reformer will generally require CO_2 removal prior to entry into a methanol or FT synthesis unit. The relative ratio of H_2 to CO or CO_2 exiting the autothermal reformer is less than the ideal stoichiometric ratio, so the synthesis gas composition must be adjusted appropriately via addition of H_2 or removal of CO_2. This is readily accomplished through the use of industrially commercialized

Table 6. Topological Information for the Optimal Solutions for the 24 Case Studies

	Case Study											
	U-1	U-10	U-50	U-200	D-1	D-10	D-50	D-200	K-1	K-10	K-50	K-200
NG conv.	SMR	SMR	ATR	ATR	SMR	SMR	ATR	ATR	SMR	SMR	ATR	ATR
NG conv. temp.	900	900	1000	1000	900	900	1000	1000	900	900	1000	1000
WGS/RGS temp.	–	–	–	–	–	–	–	–	–	–	–	–
Min Wax FT	–	–	–	–	–	–	–	–	–	–	–	–
Nom. Wax FT	–	–	–	–	–	–	–	–	Ir. rWGS	Ir. rWGS	Ir. rWGS	Ir. rWGS
FT upgrading	–	–	–	–	–	–	–	–	Fract.	Fract.	Fract.	Fract.
MTG usage	Y	Y	Y	Y	–	–	–	–	–	–	–	–
MTOD usage	–	–	–	–	Y	Y	Y	Y	–	–	–	–
CO2SEQ usage	Y	Y	Y	Y	Y	Y	Y	Y	Y	Y	Y	Y
GT usage	–	–	–	–	–	–	–	–	–	–	–	–

	R-1	R-10	R-50	R-200	A-U-1	S-U-1	P-U-1	C-U-1	U-1-Z	U-10-Z	U-50-Z	U-200-Z
NG conv.	SMR	SMR	ATR	ATR	ATR	SMR	PO	OC	SMR	SMR	ATR	ATR
NG conv. temp.	900	900	1000	1000	1000	950	450	800	900	900	1000	1000
WGS/RGS temp.	–	–	–	–	–	–	–	–	–	–	–	–
Min wax FT	–	–	–	–	–	–	–	–	–	–	–	–
Nom. wax FT	–	Ir. rWGS	Ir. rWGS	Ir. rWGS	–	–	–	–	–	–	–	–
FT upgrading	–	ZSM-5	ZSM-5	ZSM-5	–	–	–	–	–	–	–	–
MTG usage	Y	Y	Y	Y	Y	Y	Y	–	Y	Y	Y	Y
MTOD usage	Y	–	–	–	–	–	–	–	–	–	–	–
CO2SEQ usage	Y	Y	Y	Y	Y	Y	Y	Y	Y	Y	Y	Y
GT usage	–	–	–	–	–	–	–	–	–	–	–	–

The temperature of the conversion technology is selected along with the operating temperature of the reverse WGS unit (RGS), if utilized. The presence of a CO_2 sequestration system (CO2SEQ) or a GT is noted using yes (Y) or no (N). The minimum wax and maximum wax FT units are designated as either cobalt-based or iron-based units. The iron-based units will either facilitate the forward (fWGS) or reverse water-gas-shift (rWGS) reaction. The FT vapor effluent will be upgraded using fractionation into distillate and naphtha (Fract.) or ZSM-5 catalytic conversion. The use of MTG and MTO/MOGD is noted using yes (Y) or no (−).

precombustion CO_2 capture technology,[75] which can provide recycle of the CO_2 to the autothermal reformer. The extent of CO_2 recycle vs. venting or sequestration is dependent on the level of heat integration within the plant and the life cycle GHG emissions requirement. Conversely, the steam reformer will generally output a synthesis gas that has too high of a H_2 content (e.g., >5). CO_2 recycle to the reformer can also be utilized to reduce the concentration of H_2 and increase the overall carbon efficiency of the plant. However, the CO_2 will need to be recovered from an atmospheric pressure flue gas stream using postcombustion capture technology that is not as commercially prevalent as the precombustion capture technology and will require a higher level of process contingency.[75] For the autothermal reformer, any H_2 addition must be from a noncarbon-based source (i.e., electrolyzers), because the production of H_2 from natural gas will effectively decrease the overall carbon conversion yield of the process and increase the level of GHG emissions. If electrolyzers were used to produce additional H_2, note that they will also be able to provide the O_2 for the autothermal reformer and eliminate the need for an air separation unit. However, the high capital and operating costs of electrolysis generally prevent these units from being an economically competitive option. Factors that could positively impact the use of electrolyzers include (1) reducing the capital cost, (2) increasing efficiency, (3) the resale value of excess H_2 or O_2, and (4) the market value of electricity.

None of the 24 case studies utilized a dedicated reverse WGS unit for CO_2 consumption. The equilibrium constant for the WGS reaction at the expected operating temperatures of the dedicated unit make for less favorable conditions than the operating temperatures of the steam reformer or autothermal reformer. Therefore, in the 22 case studies that used a reformer to convert natural gas to synthesis gas, a portion of the CO_2 that was captured from the GTL refinery was directed to the reformer for consumption. In each of the 22 case studies, CO_2 consumption also occurred in the FT or methanol synthesis units. The reverse WGS reaction was able to occur at these lower temperatures due to the consumption of CO for the synthesis reactions. This decrease of CO provides the key driver for the consumption of CO_2 that is otherwise unavailable in a dedicated reverse WGS unit.

The 12 case studies that allowed for an unrestricted liquid product composition all selected methanol synthesis and MTG as the optimal technology. This reflects the expected reduction in capital costs associated with hydrocarbon production via methanol synthesis vs. FT synthesis that come from the reduced capital cost of methanol synthesis and MTG. Note that gasoline can be produced from FT synthesis and subsequent conversion of the hydrocarbons to gasoline via a ZSM-5 catalyst, but this process requires a higher capital investment over methanol synthesis. Both the MTG and the FT/ZSM-5 processes will produce a significant amount of byproduct LPG (9 vol %). The four case studies that maximize the diesel production utilized the methanol-to-olefins (MTO) and the MOGD processes to produce a high-quality diesel, whereas the four case studies that maximize kerosene will use a iron-based low-temperature FT synthesis followed by standard fractionation of the hydrocarbon species. The four case studies that produce liquid fuels in the ratios consistent with United States demands show a significant topological trade-off at different capacity levels. That is, at the 1 kBD capacity, methanol synthesis and subsequent conversion is the sole method for producing liquid fuels. As the capacity of the GTL refinery increases, the iron-based low-temperature FT unit is incorporated to provide the distillate products via wax hydrocracking and the gasoline product through ZSM-5 conversion. Additional gasoline is produced via the MTG route to provide the balance of the plant requirement.

In all 24 cases, CO_2 sequestration was utilized to provide a reduction in life cycle emissions for the GTL refinery. The first 20 case studies only incorporate CO_2 sequestration for a portion of the produced CO_2, while the balance of the CO_2 is either recycled back to the process or vented. In these cases, the cost of CO_2 capture may be required to meet process operating conditions or economically justified to increase the carbon yield of the process. CO_2 sequestration is solely utilized as a basis for GHG reduction and does not provide any economic benefit to the GTL refinery if a CO_2 tax is not imposed on the process. The final four case studies (U-*C*-Z) show the effect of forcing a maximum on the vented CO_2. The topological design of the units to produce the liquid fuels is equivalent to the corresponding case studies that do not impose the upper limit on the CO_2 venting (i.e., U-*C*). The only additions that are included in these last four case studies are the additional CO_2 capture/sequestration capacity and the resulting increase in the capital cost and utility requirement of the plant. For all case studies, waste heat is converted to steam for use both in the process units and in the steam cycle to provide electricity. GTs were not selected for use in any of the studies.

As an illustrative example, PFDs for the U-1 and the K-50 case studies are shown in Figures 4 and 5. These PFDs highlight the key points for natural gas conversion, hydrocarbon conversion, hydrocarbon upgrading, and CO_2 handling that are implemented in each of the 24 case studies. Note that several process units including heat exchangers, compressors, flash units, distillation columns, and turbines are not shown. The PFD for U-1 shows the natural gas conversion through steam reforming with recycle CO_2 being provided by postcombustion separation. Note that only a portion of the flue gas from the combustor is passed through the CO_2 separation unit, while the balance is sent to the stack. This split fraction is chosen so as to only capture the CO_2 that needs to be recycled or sequestered. All additional CO_2 that will be vented will simply bypass the postcombustion capture unit and flow to the stack. The heat needed for the steam reforming reaction is provided by recycle fuel gas passing over the fuel combustor unit. Therefore, no additional natural gas input is needed to provide the heat for steam reforming. The syngas exiting the steam reformer passes through the methanol synthesis section where recycle of the unreacted syngas yields an overall conversion of 94% of the CO and CO_2 to methanol. The methanol is then converted to raw hydrocarbons via a ZSM-5 catalyst, which are separated and upgraded to gasoline and LPG. All additional case studies that utilize steam reforming will implement a natural gas conversion and CO_2 handling section that is very similar to that of Figure 4. The key differences in the PFDs are found in the hydrocarbon conversion and hydrocarbon upgrading sections, which are chosen based on the composition of fuels that is desired from the plant.

The PFD for the K-50 case study (Figure 5) highlights an important difference in the natural gas conversion and the CO_2 handling associated with ATR. Specifically, the input natural gas is converted to syngas using steam and oxygen provided by the air separation unit. Precombustion capture technology is then used on the entire syngas steam to remove the CO_2 for recycle or sequestration. The resulting syngas that exits the

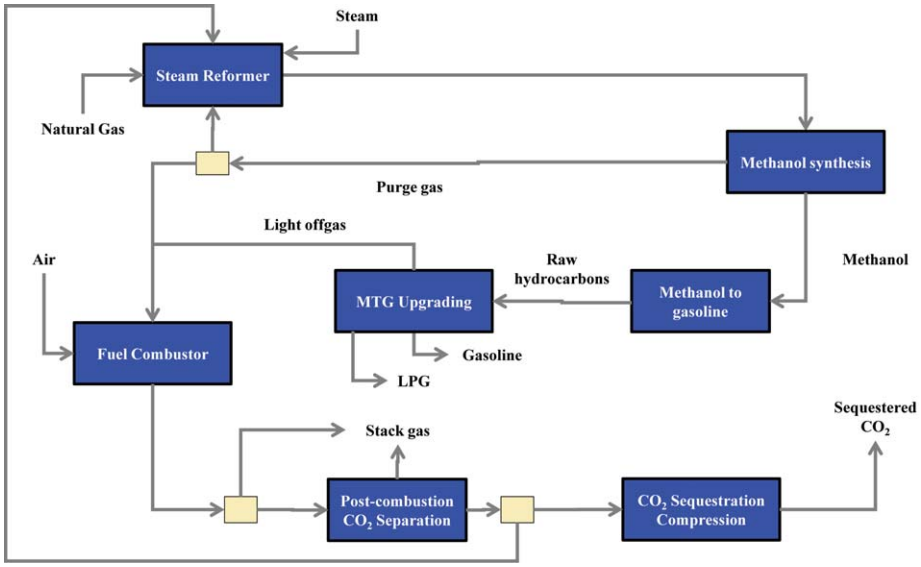

Figure 4. PFD for case study U-1.

[Color figure can be viewed in the online issue, which is available at wileyonlinelibrary.com.]

CO_2 capture unit will, therefore, have a low CO_2 concentration, and an H_2-to-CO ratio of about 2. In this case study, the syngas is converted to raw hydrocarbons via the low-temperature FT reactor, which provides a significant quantity of wax that is an ideal feedstock for distillate production. Reforming of the naphtha fraction from the FT unit will provide an aromatic-rich gasoline blendstock and an H_2-rich offgas stream. Pure H_2 that is needed for hydrocracking and hydrotreating is extracted from the H_2-rich offgas via pressure-swing adsorption. Unreacted syngas from the FT reactor is mostly recycled to the ATR unit with a portion passing over the fuel combustor to provide heat for the refinery. Postcombustion capture of the CO_2 in the stack gas is not utilized. The natural gas conversion and CO_2 handling are similar for all case studies that utilize the ATR for syngas production.

Overall costs of liquid fuels

The overall cost of liquid fuel production (in \$/GJ) is based on the costs of feedstocks, capital investment, operation and maintenance, and CO_2 sequestration and can be partially defrayed using byproduct sales of LPG and electricity. Feedstock costs are based on the as-delivered price for natural gas, butanes needed for the isomerization process,[12,14,71] and freshwater needed to make up for process losses.[15] Table 7 outlines the breakdown of the cost contribution for each case study, as well as the lower bound and the optimality gap values. The total cost is also converted into a break-even oil price (BEOP) in \$/barrel (bbl) based on the refiner's margin for gasoline, diesel, or kerosene[8,14] and represents the price of crude oil at which the GTL process becomes economically competitive

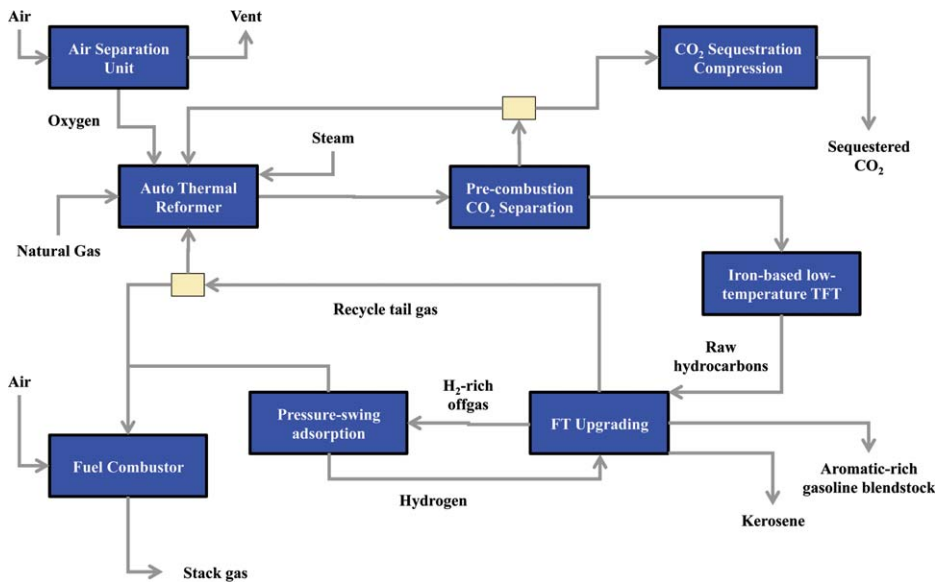

Figure 5. PFD for case study K-50.

[Color figure can be viewed in the online issue, which is available at wileyonlinelibrary.com.]

Table 7. Overall Cost Results for the 24 Case Studies

Contribution to Cost ($/GJ of Products)	Case Study															
	U-1	U-10	U-50	U-200	D-1	D-10	D-50	D-200	K-1	K-10	K-50	K-200	R-1	R-10	R-50	R-200
Natural Gas	7.67	7.60	7.81	7.75	8.13	7.93	7.96	7.78	7.62	7.44	7.71	8.14	7.62	7.62	7.59	7.60
Butane	–	–	–	–	–	–	–	–	–	–	–	–	0.35	0.35	0.31	0.29
Water	0.03	0.02	0.02	0.03	0.03	0.02	0.03	0.03	0.02	0.03	0.02	0.02	0.02	0.02	0.02	0.03
CO_2 TS&M	0.03	0.02	0.04	0.04	0.05	0.03	0.04	0.03	0.03	0.02	0.03	0.06	0.04	0.04	0.05	0.05
Investment	11.88	6.86	5.77	5.02	11.94	6.88	5.67	4.89	12.30	6.98	5.84	5.04	12.49	7.17	6.07	5.31
O&M	3.14	1.81	1.52	1.33	3.15	1.82	1.50	1.29	3.25	1.84	1.54	1.33	3.30	1.89	1.60	1.40
Electricity	−0.72	−0.74	−0.83	−0.68	−0.68	−0.74	−0.79	−0.70	−1.13	−0.94	−1.28	−1.29	−1.12	−1.12	−0.83	−0.83
LPG	−2.05	−2.05	−2.05	−2.05	−0.93	−0.85	−0.69	−0.69	–	–	–	–	−0.46	−0.46	−0.41	−0.42
Total ($/GJ)	19.97	13.53	12.27	11.44	21.68	15.10	13.72	12.63	22.08	15.38	13.86	13.30	22.24	15.52	14.39	13.43
Total ($/bbl)	101.03	64.31	57.16	52.38	110.77	73.25	65.38	59.20	113.06	74.87	66.21	63.03	114.00	75.68	69.23	63.76
Lower Bound ($/GJ)	19.08	12.81	11.73	10.85	20.51	14.42	12.97	12.01	21.01	14.88	13.11	12.73	21.59	15.07	13.93	12.79
Gap	4.46%	5.34%	4.39%	5.10%	5.37%	4.51%	5.44%	4.91%	4.85%	3.26%	5.42%	4.34%	2.95%	2.93%	3.17%	4.78%

	U-1-Z	U-10-Z	U-50-Z	U-200-Z	P-U-1	C-U-1	A-U-1	S-U-1	A-U-10	S-U-10	A-U-50	S-U-50	A-U-200	S-U-200
Natural Gas	7.67	7.60	7.81	7.75	8.13	7.82	8.15	7.67	7.71	7.60	7.81	7.92	7.75	7.70
Butane	-	-	-	-	-	-	-	-	-	-	-	-	-	-
Water	0.03	0.02	0.02	0.03	0.02	0.02	0.03	0.03	0.02	0.02	0.02	0.02	0.03	0.03
CO_2 TS&M	0.03	0.02	0.04	0.04	0.06	0.04	0.07	0.03	0.02	0.02	0.04	0.04	0.04	0.04
Investment	12.29	7.02	5.88	5.33	13.74	14.73	12.43	11.88	6.99	6.86	5.77	5.86	5.02	5.35
O&M	3.25	1.86	1.55	1.41	3.63	3.89	3.28	3.14	1.85	1.81	1.52	1.55	1.33	1.41
Electricity	−0.29	−0.30	−0.33	−0.27	−0.91	−0.75	−0.68	−0.72	−0.74	−0.74	−0.83	−0.84	−0.68	−0.69
LPG	−2.05	−2.05	−2.05	−2.05	−2.05	−2.05	−2.05	−2.05	−1.99	−2.05	−2.05	−2.08	−2.05	−2.09
Total ($/GJ)	20.92	14.18	12.92	12.22	22.62	23.70	21.22	19.97	13.86	13.53	12.27	12.46	11.44	11.74
Total ($/bbl)	106.46	68.00	60.84	56.88	116.13	122.30	108.15	101.03	66.22	64.31	57.16	58.22	52.38	54.13
Lower Bound ($/GJ)	19.89	13.54	12.49	11.80	21.53	22.94	20.02	19.16	13.06	12.81	11.73	11.97	10.85	11.18
Gap	4.92%	4.46%	3.29%	3.50%	4.81%	3.22%	5.63%	4.04%	5.78%	5.34%	4.39%	3.94%	5.10%	4.79%

The contribution to the total costs (in $/GJ) come from natural gas, butanes, water, CO_2 transportation/storage/monitoring (CO_2 TS&M), investment, and operations/maintenance (O&M). Propane and electricity are sold as byproducts (negative value). The overall costs are reported in ($/GJ) and ($/bbl) basis, along with the lower bound values in ($/GJ) and the optimality gap between the reported solution and the lower bound.

with petroleum-based processes. The lower bound found by the global optimization framework[29] is reported along with the corresponding optimality gap that ranges between 3 and 6% for each of the case studies.

The BEOP ranges between $101/bbl and $122/bbl for a 1 kBD plant, $64/bbl and $76/bbl for a 10 kBD plant, $57/bbl and $69/bbl for a 50 kBD plant, and $52/bbl and $64/bbl for a 200 kBD plant. The two major components that contribute to the overall cost are the natural gas feedstock and the costs related to capital investment (i.e., capital charges, operation, and maintenance). There is a significant economy of scale that is expected when increasing the plant capacity from 1 to 10 kBD, because a singular train (i.e., parallel combination of units) will be needed for most sections of the plant. That is, only one natural gas conversion unit (steam reformer or direct conversion), FT synthesis, methanol synthesis, or methanol conversion unit will be needed to produce the given quantity of liquid fuels. Once the capacity of the plant rises to 50 or 200 kBD, several trains will be required throughout the GTL refinery to process the large quantities of material in the plant. Some capital cost savings may be expected, because multiple units in the same train may share some auxiliary equipment, and the labor required to install the units is generally less than a linear increase.[8] However, the effect of economy of scale will be diminished for GTL plants above 10–20 kBD.

For a given capacity, Table 7 shows that the overall fuels cost will depend on the type/composition of liquid fuels produced. The unrestricted composition cases (U) tend to have the lowest overall fuels cost, followed by the max diesel cases, then the max kerosene cases, and finally the United States ratio cases. The change in the BEOP is primarily due to the change in the investment cost between these groups of case studies, which is a function of the GTL refinery complexity that is needed to produce the desired liquid fuels. For the unrestricted case studies, the sale of byproduct LPG is assumed to provide a stronger economic benefit than the other case studies. If the production of LPG from the MTG technology is not desired, the LPG may be consumed in the process to produce synthesis gas via steam reforming or ATR or converted to C_{6+} aromatics via the Cyclar process.[86] The choice of technology will ultimately depend on the available market for LPG and aromatic chemicals or the aromatics requirements of the output gasoline.

Four case studies that enforce near-zero levels of CO_2 venting show the increase in the BEOP as a result of additional CO_2 capture/sequestration installed capacity. An increase of 5–8% in the overall cost is seen over the U-*C* case studies, which is partially due to the increase in investment cost and a decrease in the sale of byproduct electricity. The four case studies that enforce one particular type of natural gas conversion technology show that the natural gas direct conversion case studies are less economically attractive than the reforming cases. This is consistent with earlier studies of direct conversion technologies,[32,64] which are limited by the low conversion of methane that is typically allowed in these processes. Improvements in the methanol yield from partial oxidation or olefins content from OC may reduce the capital investment associated with these processes to a point where it is favorable with the indirect conversion technologies. The overall cost results are included for six additional runs where either the autothermal reformer or steam reformer was fixed as the natural gas conversion technolgy. Runs A-U-*C* show how the BEOP changes for the autothermal reactor cases as capacity increases, whereas runs S-U-*C* show similar results for the

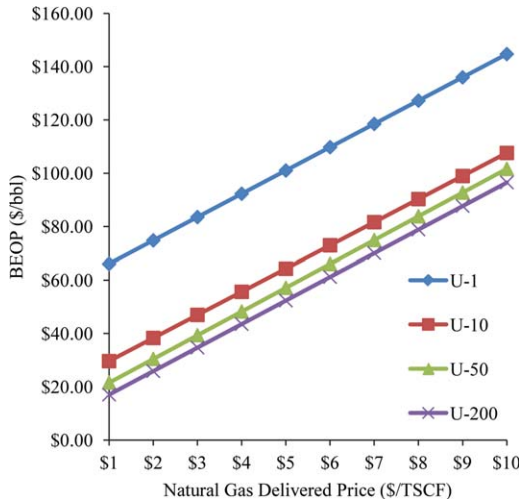

Figure 6. Parametric analysis of natural gas cost.

The BEOP is plotted for the case studies with an unrestricted product composition as a function of the natural gas price in TSCF. [Color figure can be viewed in the online issue, which is available at wileyonlinelibrary.com.]

steam reformer. For the 1 and 10 kBD case studies, the steam reformer provides a less expensive means for fuel production, whereas the autothermal reformer is more economical at 50 and 200 kBD. This is largely due to increased investment and natural gas costs associated with the autothermal reformer at low capacities and the steam reformer at higher capacities.

Parametric analysis

Table 7 indicates that the two largest contributions to the overall fuels cost are the fixed/variable capital costs (i.e., capital charges and operation/maintenance) and the natural gas purchase cost. The case studies outlined above have assumed that natural gas is available at the national average price, though this may be higher or lower throughout the country depending on the location, availability, and demand for the feedstock. Therefore, it is important to investigate how the BEOP will be effected for changing purchase costs of natural gas. As an illustrative example, the BEOP for the U-*C* case studies is calculated, assuming that natural gas is priced from \$1/thousand standard cubic feet (TSCF) to \$10/TSCF. Note that the resale value of electricity may be directly tied to the purchase price of natural gas, so the price of electricity should change accordingly with the natural gas price. Assuming that the natural gas cost is 80% of the price of electricity,[75] then the electricity will change linearly between \$0.025/kW h and \$0.126/kW h, as the natural gas price increases.

The resulting parametric analysis is plotted in Figure 6. For the 1 kBD case study, the BEOP ranges from \$70/bbl to \$143/bbl at the natural gas price increases from \$1/TSCF to \$10/TSCF. The range of BEOP for the 10 kBD case is \$33–105/bbl, \$26–99/bbl for the 50 kBD case, and \$20–94/bbl for the 200 kBD case. This analysis highlights the key economic advantages with the development of a refinery in a location with a low delivered cost of natural gas (e.g., \$1/TSCF-\$3/TSCF). Lower costs of natural gas allow for the small capacity processes outlined in this study to be constructed with significantly less economic risk. Note that the effect of changing the natural gas purchase price will be similar for other case studies with a similar capacity.

In addition, the capital costs of the units may also vary geographically or over time, and there are uncertainties associated with the nominal capital costs used in this study. Investigating the capital cost effect for each unit on the optimal topology will require a large combination of parametric study. To address this, the process synthesis approach using optimization under uncertainty will be studied as a future subject. In this article, however, a uniform increase of 5% in the unit capital costs produces a 2–3.5% increase in the overall cost of fuel production for all case studies.

Investment costs

The TPC is decomposed into cost contributions from different sections of the plant in Table 8, namely the syngas generation, syngas cleaning, hydrocarbon production, hydrocarbon upgrading, hydrogen/oxygen production, heat and power integration, and wastewater treatment sections. For the case studies that utilize indirect conversion of natural gas, the syngas generation section and the hydrocarbon production section are consistently the highest contributing factors in the investment cost. The cost of utility production (i.e., electricity and steam) generally make up the third most expensive component, with syngas cleaning (i.e., CO_2 capture and compression) and hydrocarbon upgrading following next. The values in Table 8 can be converted to a "total overnight cost" by adding the anticipated preproduction costs, inventory capital, financing costs, and other owner's costs and then to a "total as-spent capital" by figuring in capital escalation and interest on debt that occurs during construction.[75] Note that this information has been accounted for when determining the capital charge factor to use for the GTL refinery.

The TPC ranges from \$138 to \$171 MM for 1 kBD plants, \$798 to \$834 MM for 10 kBD plants, \$3354 to \$3527 MM for 50 kBD plants, and \$11,384 to \$12,387 MM for 200 kBD plants. The normalized investment costs reveal the economies of scale obtained at the different capacity levels and range from \$138k to \$171k/bpd for 1 kBD, \$80k to \$84k/bpd for 10 kBD plants, \$67k to \$70k/bpd for 50 kBD plants, and \$58k to \$62k/bpd for 200 kBD plants. Among the case studies, the plants with an unrestricted fuel requirement and the max diesel cases both provide similar TPCs. The increased costs associated with hydrogen production and a more complicated hydrocarbon refining section for the max diesel cases are balanced by an overall increase in the gas capacity required in the unrestricted cases. The LPG produced in the refineries is not added to the total plant capacity, because this is not considered to be a liquid transportation fuel and is merely a byproduct. Therefore, the plants that utilize the MTG technology must have higher capacities for natural gas conversion and methanol synthesis, because ~10% of the carbon in the process will leave as LPG. The increase in costs for the max kerosene and the United States ratio cases is mostly associated with the use of FT synthesis and the upgrading of the hydrocarbon products, though these two sets of case studies are typically 3–6% higher than the case studies that utilize methanol synthesis.

The driving factor for the selection of steam reforming or ATR of natural gas as the preferred route in all the case studies is most clearly illustrated in case studies A-U-1, S-U-1, P-U-1, and C-U-1, where the natural gas conversion technology is imposed in each case study. In Table 8, the case studies that utilize direct conversion of natural gas (i.e., P-U-

Table 8. Breakdown of the Investment Costs for the 24 Case Studies

	Case Study											
Contribution to Cost (MM $)	U-1	U-10	U-50	U-200	D-1	D-10	D-50	D-200	K-1	K-10	K-50	K-200
Syngas generation	53	318	1361	4439	48	288	1164	4152	54	287	1158	3736
Syngas cleaning	10	57	242	830	8	47	215	763	8	47	195	666
Hydrocarbon production	39	224	926	3450	39	215	907	2942	40	236	997	3583
Hydrocarbon upgrading	11	59	266	904	14	79	326	1190	13	74	336	1243
Hydrogen/oxygen production	–	–	–	–	8	48	190	634	8	47	210	685
Heat and power integration	19	112	443	1654	17	98	387	1311	16	95	384	1432
Wastewater treatment	5	28	116	408	4	25	110	392	5	25	113	387
Total (MM $)	138	798	3354	11685	139	800	3299	11384	143	812	3393	11732
Total ($/bpd)	138,127	79,808	67,072	58,427	138,799	79,997	65,977	56,922	142,978	81,192	67,866	58,658

	R-1	R-10	R-50	R-200	A-U-1	S-U-1	P-U-1	C-U-1	U-1-Z	U-10-Z	U-50-Z	U-200-Z
Syngas generation	49	278	1165	4067	50	53	–	–	53	308	1324	4589
Syngas cleaning	9	50	227	771	10	10	5	5	15	88	368	1202
Hydrocarbon production	40	232	995	3512	38	39	67	122	39	219	917	3558
Hydrocarbon upgrading	16	93	388	1259	11	11	56	23	11	60	260	927
Hydrogen/oxygen production	8	51	208	763	11	–	11	–	–	–	–	–
Heat and power integration	18	104	436	1628	19	19	17	17	19	114	438	1702
Wastewater treatment	5	26	107	348	5	5	4	5	5	28	114	408
Total (MM $)	145	834	3527	12,347	144	138	160	171	143	817	3420	12,387
Total ($/bpd)	145,227	83,393	70,538	61,736	144,488	138,127	159,744	171,327	142,900	81,657	68,408	61,933

The major sections of the plant include the syngas generation section, syngas cleaning, hydrocarbon production, hydrocarbon upgrading, hydrogen/oxygen production, heat and power integration, and wastewater treatment blocks. The values are reported in MM $ and normalized with the amount of fuels produced ($/bpd).

1 and C-U-1) have higher hydrocarbon production/upgrading costs. For the OC case (i.e, C-U-1), the cost of olefins production is much higher than that for hydrocarbon production from the indirect cases due to low conversion rates of methane and the subsequent high costs of compression for the recycle gases. The units utilized in this topology include the olefin fractionation (MTO-F), olefins to gasoline to distillate (OGD), hydrocarbon fractionation (MTODF), distillate and kerosene hydrotreaters (DHT, KHT), and the units in the LPG–gasoline separation section (see Supporting Information, Figures S7 and S8). The effect of the low conversion is the high flow rate of recycle gases in Supporting Information, Figure S8 that increase the volumetric flow rate for the CO_2 separation (see Supporting Information, Table S1) and compression to recycle the gases to various process units. Similarly, the low selectivity of methanol in the partial oxidation of natural gas (case study P-U-1) has the same effect on the hydrocarbon production and upgrading costs. The off-gas stream in Supporting Information, Figure S7 is high, increasing the capital cost of the subsequent units. For the case studies enforcing a CO_2 venting maximum, note that the majority of the cost increase is associated with the syngas cleaning as a result of additional CO_2 capture/compression capacity. In general, this results in an increase of about 5% to the TPC from the other unrestricted case studies (U-*C*).

Material and energy balances

The overall material and energy balances for the 24 case studies are shown in Tables 9 and 10, respectively. The natural gas is shown in million standard cubic feet per hour (mscf/h), whereas the butane, liquid products, and water are shown in kBD. For all the plants of a given capacity, a similar quantity of natural gas needed, which is consistent with the cost results in Table 7. The major differences between the case studies are based on the type and quantity of liquid fuels that are produced along with the amount of CO_2 that is sequestered and vented. For the unrestricted case studies, the refinery capacity is solely dedicated to the production of gasoline through the MTG process, with a byproduct amount of LPG that is approximately equal to 9 vol % of the total gasoline. The case studies that maximized diesel production were forced to have at least 75 vol % of the liquid product be diesel. All the case studies produced exactly 75 vol % diesel, 25 vol % gasoline, and about 3–5 v/v% byproduct LPG. For the maximum kerosene cases (i.e., at least 75 vol % kerosene), 75 vol % of the products is kerosene, and 25 vol % is an aromatic-rich gasoline blendstock. No byproduct LPG is produced in these cases, as the Cyclar process[86] was used to increase the yield of gasoline and kerosene-range aromatics from the refinery. For these latter sets of case studies, higher volumetric percentages of diesel or kerosene could be obtained through refining of the gasoline fraction, though the resulting GTL refineries would be less economically attractive. The composition of the liquid fuels from the United States ratios case studies was fixed for each refinery to be approximately 67 vol % gasoline, 22 vol % diesel, and 11 vol % kerosene. The total amount of LPG formed as a byproduct for these cases is equal to 2 vol % of the total gasoline/diesel/kerosene produced.

Variations in the amount of sequestered and vented CO_2 can be observed across the 24 case studies. For the unrestricted case studies and the maximum kerosene case studies, the amount of vented CO_2 represents ~75% of the total CO_2 that is output from the process. The United States ratio studies show a decrease in the vented CO_2 to about 67% of the total, whereas the maximum diesel cases are around 60–65%. It is important to note that the amount of CO_2 sequestration that is utilized is directly a function of the life cycle GHG emissions that are required from the process. If no restriction was placed on the life cycle emissions, then all of the CO_2 that is output from the refinery would simply be vented, resulting in a decrease in the capital and utility costs of the plant. For the near-zero emissions case studies, a

Table 9. Overall Material Balance for the 24 Case Studies

	Case Study											
Material Balances	U-1	U-10	U-50	U-200	D-1	D-10	D-50	D-200	K-1	K-10	K-50	K-200
Natural gas (mscf/h)	0.36	3.61	18.53	73.57	0.39	3.76	18.89	73.85	0.36	3.54	18.31	77.28
Butane (kBD)	–	–	–	–	–	–	–	–	–	–	–	–
Water (kBD)	1.92	14.01	74.21	400.25	1.80	17.34	90.89	406.92	1.42	19.85	85.89	300.19
Gasoline (kBD)	1.00	10.00	50.00	200.00	0.25	2.50	12.50	50.00	0.25	2.50	12.50	50.00
Diesel (kBD)	–	–	–	–	0.75	7.50	37.50	150.00	–	–	–	–
Kerosene (kBD)	–	–	–	–	–	–	–	–	0.75	7.50	37.50	150.00
LPG (kBD)	0.09	0.90	4.50	19.78	0.04	0.37	1.52	6.06	–	–	–	–
Seq. CO_2 (tonne/h)	1.36	10.98	84.64	347.18	2.34	16.53	91.88	265.71	1.35	10.00	73.66	587.99
Vented CO_2 (tonne/h)	4.03	40.99	204.30	796.88	3.40	35.64	176.63	706.08	4.15	40.14	214.71	808.07

	R-1	R-10	R-50	R-200	A-U-1	S-U-1	P-U-1	C-U-1	U-1-Z	U-10-Z	U-50-Z	U-200-Z
Natural gas (mscf/h)	0.36	3.62	18.02	72.20	0.39	0.36	0.39	0.37	0.36	3.61	18.53	73.57
Butane (kBD)	0.03	0.26	1.14	4.29	–	–	–	–	–	–	–	–
Water (kBD)	1.68	16.84	63.37	370.23	1.78	1.92	1.78	1.43	1.92	14.01	74.21	400.25
Gasoline (kBD)	0.67	6.72	33.60	134.39	1.00	1.00	1.00	1.00	1.00	10.00	50.00	200.00
Diesel (kBD)	0.22	2.15	10.77	43.10	–	–	–	–	–	–	–	–
Kerosene (kBD)	0.11	1.13	5.63	22.51	–	–	–	–	–	–	–	–
LPG (kBD)	0.02	0.16	0.74	3.01	0.09	0.09	0.10	0.10	0.09	0.90	4.50	19.78
Seq. CO_2 (tonne/h)	2.02	20.25	114.88	463.60	3.07	1.36	2.76	1.88	5.33	51.46	286.05	1132.61
Vented CO_2 (tonne/h)	3.86	38.59	174.36	696.58	3.65	4.03	4.05	4.04	0.05	0.52	2.89	11.44

The inputs to the GTL refinery are natural gas, butane, and water, whereas the outputs include gasoline, diesel, kerosene, LPG, sequestered CO_2, and vented CO_2.

significant increase in the amount of sequestered CO_2 is utilized to meet the restriction imposed on these studies.

The electricity production ranges from 1 to 4 MW for 1 kBD plants, 10 to 38 MW for 10 kBD plants, 57 to 218 MW for 50 kBD plants, and 315 to 878 MW for 200 kBD plants. In all cases, the maximum kerosene studies yield the topologies with highest producing electricity, which helps lower the overall fuels cost. The smallest amount of electricity is produced from the near-zero CO_2 venting case studies, which is anticipated due to the higher utility demand for these plants. In general, the electricity output from all the case studies improves the efficiency of the topologies, with the U-10, D-200, and K-10 case studies achieving the highest energy efficiencies (i.e., 75.6, 75.0, and 75.7%, respectively) compared with other case studies in their subcategories (see Table 10). The energy efficiency values are calculated by dividing the total energy output (i.e., fuel products, propane, or electricity) by the total energy input (i.e., natural gas or butane). As electricity is output from the system in all case studies, the value is listed as negative in Table 9, and the magnitude of the energy value in Table 10 is added to the total output. If electricity were to be input to the GTL refineries, then this energy value would be added to the total input to the system. The overall energy efficiency of the GTL refineries is above 75.0% for all plant sizes.

Table 10. Overall Energy Balance for the 24 Case Studies

	Case Study											
Energy Balances (MW)	U-1	U-10	U-50	U-200	D-1	D-10	D-50	D-200	K-1	K-10	K-50	K-200
Natural gas	97	958	4918	19,524	102	999	5013	19,599	96	938	4858	20,510
Butane	–	–	–	–	–	–	–	–	–	–	–	–
Gasoline	64	644	3219	12,743	16	159	796	3186	16	159	796	3186
Diesel	–	–	–	–	53	533	2667	10,668	–	–	–	–
Kerosene	–	–	–	–	–	–	–	–	52	519	2596	10,384
LPG	5	55	273	1202	2	23	92	368	–	–	–	–
Electricity	−2	−25	−141	−460	−2	−25	−134	−475	−4	−32	−218	−878
Efficiency (%)	74.8	75.6	73.9	73.8	72.3	74.1	73.6	75.0	74.7	75.7	74.3	70.4

	R-1	R-10	R-50	R-200	A-U-1	S-U-1	P-U-1	C-U-1	U-1-Z	U-10-Z	U-50-Z	U-200-Z
Natural gas	96	960	4782	19,159	103	97	102	98	97	958	4918	19,524
Butane	2	16	69	260	–	–	–	–	–	–	–	–
Gasoline	43	428	2141	8563	64	64	64	64	64	644	3219	12,743
Diesel	15	153	766	3065	0	0	0	0	–	–	–	–
Kerosene	8	78	390	1558	0	0	0	0	–	–	–	–
LPG	1	10	45	183	6	5	6	6	5	55	273	1202
Electricity	−4	−38	−141	−563	−2	−2	−3	−3	−1	−10	−57	−315
Efficiency (%)	72.5	72.5	71.8	71.7	70.2	74.8	71.1	73.4	73.3	74.0	72.2	73.0

The energy inputs to the GTL refinery come from natural gas and butane, and the energy outputs are gasoline, diesel, kerosene, LPG, and electricity. The energy efficiency of the process is calculated by dividing the total energy output with the total energy inputs to the process.

Table 11. Carbon Balances (in kg/s) for the Optimal Solutions for the 24 Case Studies

	Case Study											
	U-1	U-10	U-50	U-200	D-1	D-10	D-50	D-200	K-1	K-10	K-50	K-200
Natural gas	1.65	16.34	83.88	333.01	1.75	17.04	85.51	334.29	1.64	16.00	82.86	349.81
Butane	–	–	–	–	–	–	–	–	–	–	–	–
Gasoline	1.17	11.73	58.64	231.63	0.29	2.90	14.48	57.91	0.29	2.90	14.48	57.91
Diesel	–	–	–	–	0.99	9.91	49.56	198.23	–	–	–	–
Kerosene	–	–	–	–	–	–	–	–	0.93	9.30	46.52	186.08
LPG	0.07	0.67	3.33	14.66	0.03	0.28	1.12	4.49	–	–	–	–
Vented CO_2	0.31	3.11	15.49	60.41	0.26	2.70	13.39	53.52	0.31	3.04	16.28	61.25
Seq. CO_2	0.10	0.83	6.42	26.32	0.18	1.25	6.96	20.14	0.10	0.76	5.58	44.57
% conversion	75.2	75.9	73.9	74.0	75.1	76.8	76.2	78.0	74.5	76.2	73.6	69.7

	R-1	R-10	R-50	R-200	A-U-1	S-U-1	P-U-1	C-U-1	U-1-Z	U-10-Z	U-50-Z	U-200-Z
Natural gas	1.64	16.37	81.56	326.78	1.75	1.65	1.75	1.68	1.65	16.34	83.88	333.01
Butane	0.02	0.23	1.04	3.92	–	–	-	–	–	–	–	–
Gasoline	0.78	7.78	38.91	155.64	1.17	1.17	1.17	1.17	1.17	11.73	58.64	231.63
Diesel	0.28	2.85	14.24	56.95	–	–	–	–	–	–	–	–
Kerosene	0.14	1.40	6.98	27.93	–	–	–	–	–	–	–	–
LPG	0.01	0.12	0.55	2.23	0.07	0.07	0.07	0.07	0.07	0.67	3.33	14.66
Vented CO_2	0.29	2.93	13.22	52.80	0.28	0.31	0.31	0.31	0.00	0.04	0.22	0.87
Seq. CO_2	0.15	1.53	8.71	35.14	0.23	0.10	0.21	0.14	0.40	3.90	21.68	85.86
% conversion	73.1	73.1	73.5	73.4	70.9	75.2	71.3	74.2	75.2	75.9	73.9	74.0

Carbon is input to the process via natural gas or butanes and exits the process as liquid product, LPG byproduct, vented CO_2, or sequestered (Seq.) CO_2. The small amount of CO_2 input to the system in the purified oxygen stream ($< 0.01\%$) is neglected.

Carbon and GHG balances

The overall carbon balance for the GTL refineries is shown in Table 11 and highlights the eight major points where carbon is either input or output from the system. Carbon that is input to the system via air is neglected due to the low flow rate relative to the other eight points. Over 99% of the input carbon is supplied from the natural gas, whereas the balance is supplied by the butane input to the isomerization and alkylation units. The trends seen in liquid fuel production from Table 9 are consistently displayed in the output carbon flow rates in Table 11. As the percentage of carbon in each of the liquid products is relatively similar, this implies that the relative rates of carbon flow associated with each fuel will be consistent with the volumetric flow rate of each product. The output amount of carbon in the total gasoline, diesel, and kerosene products is, therefore, approximately constant for each plant capacity. The amount of carbon leaving as LPG is around 2–7% of that leaving as gasoline, kerosene, and diesel.

For each of the case studies, the carbon conversion rate ranges from 69.7 to 78.0%, with most of the case studies achieving a conversion rate above 70%. The high conversion rates are attributed to two key factors in the GTL refinery, namely the high hydrogen/carbon ratio associated with natural gas and the utilization of CO_2 recycle to increase the overall yield. The first factor is important for the production of a syngas with enough H_2 to convert the CO and CO_2 in the gas with minimal need for CO_2 capture. In fact, the H_2 content associated with steam reforming of natural gas is high enough to allow for input of CO_2 directly into the reformer to help decrease the process CO_2. This second factor is vital for decreasing the capital requirement of all units due to higher carbon yield and for reducing the CO_2 sequestration requirement needed to achieve a proper life cycle GHG target.

The life cycle GHG emission balances for the case studies are shown in Table 12. For each of the studies, the total GHG emission target was set to be at most equal to that for petroleum-based production of liquid fuels or natural gas-based production of electricity. For each liquid product, the amount of GHG produced is calculated by determining the level of CO_2 that would be produced from complete combustion of the product. The life cycle GHG emissions (LGHG) was set to be the sum of the total emissions from each stage of the process. The GHG emissions avoided from liquid fuels (GHGAF) are equivalent to the total energy of fuels produced multiplied by a typical petroleum-based emissions level (i.e., 91.6 kg CO_{2eq}/GJ^{LHV}), whereas the GHG emissions avoided from electricity (GHGAE) are equivalent to the energy produced by electricity multiplied by a typical natural gas-based emissions level (i.e., 101.3 kg CO_{2eq}/GJ). The GHG emissions index (GHGI) represents the division of LGHG by the sum of GHGAF and GHGAE, and values less than unity are indicative processes with superior life cycle GHG emissions than current processes.

The GHG emission rates (in kg CO_2eq/s) for the eight major point sources in the refinery are listed in Table 12 and include (a) acquisition and transportation of the natural gas and butane feeds, (b) transportation and use of the gasoline, diesel, kerosene, and LPG, (c) transportation and sequestration of any CO_2, and (d) venting of any process emissions. The GHG emissions for feedstock acquisition and transportation in (a), product transportation in (b), and CO_2 transportation in (c) are calculated from the GREET model for well-to-wheel emissions[87] and assuming transportation distances for feedstocks (50 miles), products (100 miles), and CO_2 (50 miles). The GHG emissions from product use in (b) are calculated assuming that each product will be completely combusted to generate CO_2 that is simply vented to the atmosphere.

For each of the first 20 case studies, the GHGI is exactly equal to 1, implying that each of the GTL refineries has emission levels that are exactly equal to current processes. From Table 12, it is clear that a major component of the life cycle emissions are attributed to the liquid fuels. In fact, $\sim$70% of the life cycle GHG emissions result from

Table 12. GHG Balances for the Optimal Solutions for the 24 Case Studies

	Case Study											
	U-1	U-10	U-50	U-200	D-1	D-10	D-50	D-200	K-1	K-10	K-50	K-200
Natural gas	0.97	9.58	49.19	195.28	1.02	9.99	50.14	196.03	0.96	9.38	48.59	205.14
Butane	–	–	–	–	–	–	–	–	–	–	–	–
Gasoline	4.30	42.98	214.89	848.79	1.06	10.61	53.05	212.20	1.06	10.61	53.05	212.20
Diesel	–	–	–	–	3.63	36.32	181.60	726.39	–	–	–	–
Kerosene	–	–	–	–	–	–	–	–	3.41	34.09	170.47	681.88
LPG	0.24	2.44	12.22	53.71	0.11	1.01	4.12	16.46	–	–	–	–
Vented CO_2	1.12	11.39	56.75	221.35	0.95	9.90	49.06	196.13	1.15	11.15	59.64	224.47
Seq. CO_2	0.02	0.15	1.18	4.82	0.03	0.23	1.28	3.69	0.02	0.14	1.02	8.17
LGHG	6.65	66.54	334.22	1323.96	6.81	68.06	339.25	1350.90	6.60	65.38	332.77	1331.85
GHGAF	6.40	63.98	319.92	1277.36	6.57	65.53	325.70	1302.79	6.21	62.15	310.74	1242.96
GHGAE	0.25	2.56	14.31	46.60	0.23	2.53	13.55	48.12	0.39	3.23	22.03	88.89
GHGI	1.00	1.00	1.00	1.00	1.00	1.00	1.00	1.00	1.00	1.00	1.00	1.00

	R-1	R-10	R-50	R-200	A-U-1	S-U-1	P-U-1	C-U-1	U-1-Z	U-10-Z	U-50-Z	U-200-Z
Natural gas	0.96	9.60	47.83	191.63	1.03	0.97	1.02	0.99	0.97	9.58	49.19	195.28
Butane	0.00	0.03	0.13	0.47	–	–	–	–	–	–	–	–
Gasoline	2.85	28.52	142.59	570.35	4.24	4.30	4.24	4.24	4.30	42.98	214.89	848.79
Diesel	1.04	10.43	52.17	208.70	–	–	–	–	–	–	–	–
Kerosene	0.51	5.12	25.58	102.34	–	–	–	–	–	–	–	–
LPG	0.04	0.45	2.02	8.17	0.27	0.24	0.27	0.27	0.24	2.44	12.22	53.71
Vented CO_2	1.07	10.72	48.43	193.49	1.04	1.12	1.13	1.12	0.01	0.14	0.80	3.18
Seq. CO	0.03	0.28	1.60	6.44	0.04	0.02	0.04	0.03	0.13	1.30	6.49	25.96
LGHG	6.51	65.15	320.35	1281.59	6.62	6.65	6.70	6.65	5.65	55.20	277.22	1108.86
GHGAF	6.13	61.31	306.11	1224.61	6.39	6.40	6.39	6.39	6.39	63.87	319.34	1277.36
GHGAE	0.38	3.84	14.25	56.98	0.23	0.25	0.31	0.26	0.10	1.02	5.72	31.91
GHGI	1.00	1.00	1.00	1.00	1.00	1.00	1.00	1.00	0.87	0.85	0.85	0.85

The total GHG emissions (in CO_2 equivalents—kg CO_2eq/s) for feedstock acquisition and transportation, product transportation and use, CO_2 sequestration, and process venting are shown for each study. Process feedstocks include natural gas and butane, whereas products include gasoline, diesel, kerosene, and LPG.

combustion of these fuels in light and heavy duty vehicles. The remaining emissions are mostly attributed to acquisition and transportation of the natural gas and process venting. Natural gas is a particularly GHG intensive feedstock due to the small amount of methane that is leaked to the atmosphere during extraction from the ground. Nevertheless, it is still economical to develop GTL processes that can have appropriate GHG emissions targets. The last four case studies provide an indication on how low the life cycle GHG emissions can be for GTL processes. The studies have GHGI values between 0.85 and 0.87, indicating that the life cycle GHG emissions are 13–15% lower than current fossil-fuel processes. In fact, these values are close to the upper bound of GHG emissions reduction for GTL processes that do not produce a significant amount of byproduct electricity. Coproduction of liquid fuels and electricity at similar energy levels will have lower values for GHGI, as almost all of the carbon used to produce electricity can be captured and sequestered. When producing liquid fuels, it is currently not economical to provide on-board carbon capture for transportation vechiles, so the life cycle GHG emissions reduction will have a theoretical upper limit. Note that the introduction of a biomass feedstock to the refinery would allow the refinery to achieve significantly lower levels of life cycle GHG emissions.

Conclusions

This study has detailed the development of an optimization-based framework for the process synthesis of a thermochemical natural gas to liquids refinery. The framework was used to analyze multiple natural gas conversion technologies, hydrocarbon production technologies, and hydrocarbon upgrading technologies to directly compare the technoeconomic and environmental benefits of each approach. The framework also included a simultaneous heat, power, and water integration to compare the costs of utility generation and wastewater treatment in the overall cost of liquid fuels. The proposed optimization model was tested using 24 distinct case studies that are derived from four combinations of products and four plant capacities with restrictions placed on the natural gas conversion technology and the amount of CO_2 vented. The overall conversion of carbon from feedstock to liquid products was consistently found to be over 70%, and the life cycle GHG emissions was equivalent or less than current fossil-fuel processes. Each case study was globally optimized using a branch-and-bound global optimization algorithm to theoretically guarentee that the cost associated with the optimal design was within 3–6% of the best value possible.

The overall cost of liquid fuels production ranges between \$101/bbl and \$122/bbl for a 1 kBD plant, \$64/bbl and \$76/bbl for a 10 kBD plant, \$57/bbl and \$69/bbl for a 50 kBD plant, and \$52/bbl and \$64/bbl for a 200 kBD plant. The variation in the cost for each capacity is largely due to the refinery complexity needed to produce a desired quantity of liquid fuels. To minimize the overall costs of fuel production, methanol synthesis and the subsequent MTG route provides the optimal conversion pathway. A significant portion of the produced CO_2 can be recycled back to the reformer, and overall carbon conversion percentages of 70% are readily obtainable. Although this pathway assumes that about 10 vol % of the liquid product from the plant will be LPG, the MTG pathway still remains economically superior if the LPG can be refined to aromatic chemicals using the Cyclar process or co-reformed with the natural gas.

In general, the overall costs with hydrocarbon production through methanol synthesis are lower than those through FT synthesis due to the simplicity of the unconverted synthesis gas recycle loop and decrease in complexity that is required for hydrocarbon upgrading. The unreacted synthesis gas from methanol synthesis may be directly recycled to the methanol synthesis unit without a concern for byproduct species that are generated in the unit. However, the unreacted synthesis gas from FT synthesis will contain C_1—C_4 hydrocarbon species that must be separated out via distillation using refrigeration or recycled back to a reformer to prevent build-up of these species in the recycle gas loop. The benefit associated with FT synthesis is the diversity of products that can be obtained from the process. The range of C_1—C_{30+} hydrocarbons allows for a diverse array of fuels, chemicals, lubricants, and waxes that can be readily produced through standard refining practices. The process synthesis framework outlined in this study is of significant benefit, because it marks the first work in the scientific literature that is capable of accessing the technoeconomic and environmental trade-offs with multiple GTL technologies when given a desired production capacity and composition.

Acknowledgments

The authors acknowledge financial support from the National Science Foundation (NSF EFRI-0937706 and NSF CBET-1158849).

Literature Cited

1. Energy Information Administration. Monthly Energy Review—May 2012. Document Number: DOE-EIA-0035(2012/05), 2012. Available at: http://www.eta.doe.gov/mer/. Accessed Aug. 2012
2. Energy Information Administration. Annual Energy Outlook 2013 with Projections to 2035. Document Number: DOE/EIA-0383(2012), 2011. Available at: http://www.eta.doe.gov/oiaf/aeo/. Accessed Aug. 2012.
3. Floudas CA, Elia JA, Baliban RC. Hybrid and single feedstock energy processes for liquid transportation fuels: a critical review. *Comp Chem Eng*. 2012;41:24–51.
4. Lynd LR, Larson E, Greene N, Laser M, Sheehan J, Dale BE, McLaughlin S, Wang M. The role of biomass in America's energy future: framing the analysis. *Biofuels Bioprod Biorefin*. 2009;3(2):113–123.
5. Department of Energy. Biomass as Feedstock for a Bioenergy and Bioproducts Industry: The Technical Feasibility of a Billion-Ton Annual Supply. Document Number: DOE/GO-102005-2135, 2005. Available at: http://www1.eere.energy.gov/biomass/publications.html. Accessed Aug. 2012.
6. National Research Council. Water Implications of Biofuels Production in the United States. National Research Council, 2008. Available at: http://www.nap/edu/catalog/12039.html. The National Academies Press, Washington, DC. Last Accessed Aug. 2012.
7. de Fraiture C, Giordano M, Liao Y. Biofuels and implications for agricultural water use: blue impacts of green energy. *Water Policy*. 2008;10:67–81.
8. Kreutz TG, Larson ED, Liu G, Williams RH. Fischer–Tropsch fuels from coal and biomass. In: Proceedings of the 25th International Pittsburg Coal Conference, 2008. Pittsburgh, PA, 29 Sept.–2 Oct., 2008.
9. de Klerk A. Fischer-Tropsch Refining. Weinheim, Germany: Wiley-VCH, 2011.
10. National Academy of Sciences, National Academy of Engineering, and National Research Council. Liquid Transportation Fuels from Coal and Biomass: Technological Status, Costs, and Environmental Issues. Prepublication.Washington, DC: EPA, 2009.
11. Agrawal R, Singh NR, Ribeiro FH, Delgass WN. Sustainable fuel for the transportation sector. *Proc Natl Acad Sci USA*. 2007;104:4828–4833.
12. Baliban RC, Elia JA, Floudas CA. Toward novel biomass, coal, and natural gas processes for satisfying current transportation fuel demands. 1. Process alternatives, gasification modeling, process simulation, and economic analysis. *Ind Eng Chem Res*. 2010;49:7343–7370.
13. Elia JA, Baliban RC, Floudas CA. Toward novel biomass, coal, and natural gas processes for satisfying current transportation fuel demands. 2. Simultaneous heat and power integration. *Ind Eng Chem Res*. 2010;49:7371–7388.
14. Baliban RC, Elia JA, Floudas CA. Optimization framework for the simultaneous process synthesis, heat and power integration of a thermochemical hybrid biomass, coal, and natural gas facility. *Comp Chem Eng*. 2011;35:1647–1690.
15. Baliban RC, Elia JA, Floudas CA. Simultaneous process synthesis, heat, power, and water integration of thermochemical hybrid biomass, coal, and natural gas facilities. *Comp Chem Eng*. 2012;37:297–327.
16. Peng XD, Wang AW, Toseland BA, Tij PJA. Single-step syngas-to-dimethyl ether processes for optimal productivity, minimal emissions, and natural gas-derived syngas. *Ind Eng Chem Res*. 1999;38:4381–4388.
17. Sudiro M, Bertucco A. Synthetic fuels by a limited CO_2 emission process which uses both fossil and solar energy. *Energy Fuels*. 2007;21:3668–3675.
18. Cao Y, Gao Z, Jin J, Zhou H, Cohron M, Zhao H, Liu H, Pan W. Synthesis gas production with an adjustable H_2/CO ratio through the coal gasification process: effects of coal ranks and methane addition. *Energy Fuels*. 2008;22(3):1720–1730.
19. Zhou L, Hu S, Li Y, Zhou Q. Study on co-feed and co-production system based on coal and natural gas for producing dme and electricity. *Chem Eng J*. 2008;136:31–40.
20. Sudiro M, Bertucco A. Production of synthetic gasoline and diesel fuel by alternative processes using natural gas and coal: process simulation and optimization. *Energy*. 2009;34:2206–2214.
21. Zhou L, Hu S, Chen D, Li Y, Zhu B, Jin Y. Study on systems based on coal and natural gas for producing dimethyl ether. *Ind Eng Chem Res*. 2009;48:4101–4108.
22. Adams TA II, Barton PI. Combining coal gasification and natural gas reforming for efficient polygeneration. *Fuel Proc Technol*. 2011;92:639–655.
23. Adams TA II, Barton PI. Combining coal gasification, natural gas reforming, and solid oxide fuel cells for efficient polygeneration with CO_2 capture and sequestration. *Fuel Proc Technol*. 2011;92(10):2105–2115.
24. Li Z, Liu P, He F, Wang M, Pistikopoulos EN. Simulation and exergoeconomic analysis of a dual-gas sourced polygeneration process with integrated methanol/DME/DMC catalytic synthesis. *Comp Chem Eng*. 2011;35(9):1857–1862.
25. Borgwardt RH. Biomass and natural gas as co-feedstocks for production of fuel for fuel-cell vehicles. *Biomass Bioenergy*. 1997;12(5):333–345.
26. Dong Y, Steinberg M. Hynol—an economical process for methanol production from biomass and natural gas with reduced CO_2 emission. *Int J Hydrogen Energy*. 1997;22(10–11):971–977.
27. Li H, Hong H, Jin H, Cai R. Analysis of a feasible polygeneration system for power and methanol production taking natural gas and biomass as materials. *Appl Energy*. 2010;87:2846–2853.
28. Liu G, Williams RH, Larson ED, Kreutz TG. Design/economics of low-carbon power generation from natural gas and biomass with synthetic fuels co-production. *Energy Procedia*. 2011;4:1989–1996.
29. Baliban RC, Elia JA, Misener R, Floudas CA. Global optimization of a MINLP process synthesis model for thermochemical based conversion of hybrid coal, biomass, and natural gas to liquid fuels. *Comp Chem Eng*. 2012;42:64–86.
30. Baliban RC, Elia JA, Weekman VW, Floudas CA. Process synthesis of hybrid coal, biomass, and natural gas to liquids via Fischer–Tropsch synthesis, ZSM-5 catalytic conversion, methanol synthesis, methanol-to-gasoline, and methanol-to-olefins/distillate technologies. *Comp Chem Eng*. 2012;47:29–56.
31. Fox JM, Chen TP, Degen BD. Direct Methane Conversion Process Evaluations. Contract No. DE-AC22-87PC79814, 1988.
32. Gradassi MJ, Green NW. Economics of natural gas conversion processes. *Fuel Proc Technol*. 1995;42:65–83.
33. Iandoli CL, Kjelstrup S. Exergy analysis of a GTL process based on low-temperature slurry F–T reactor technology with a cobalt catalyst. *Energy Fuels*. 2007;21:2317–2324.
34. Gao L, Li H, Chen B, Jin H, Lin R, Hong H. Proposal of a natural gas-based polygeneration system for power and methanol production. *Energy*. 2008;33:206–212.
35. Hao X, Djatmiko ME, Xu Y, Wang Y, Chang J, Li Y. Simulation analysis of a gas-to-liquid process using Aspen Plus. *Chem Eng Technol*. 2008;31(2):188–196.

36. Lee CJ, Lim Y, Kim HS, Han C. Optimal gas-to-liquid product selection from natural gas under uncertain price scenarios. *Ind Eng Chem Res*. 2009;48:794–800.
37. Kim YH, Jun KW, Joo H, Han C, Song IK. A simulation study on gas-to-liquid (natural gas to Fischer–Tropsch synthetic fuel) process optimization. *Chem Eng J*. 2009;155:427–432.
38. Bao B, El-Halwagi MM, Elbashir NO. Simulation, integration, and economic analysis of gas-to-liquid process. *Fuel Proc Technol*. 2010;91:703–713.
39. Dillerop C, vander Berg H, vander Ham AGJ. Novel syngas production techniques for GTL-FT synthesis of gasoline using reverse flow catalytic membrane reactors. *Ind Eng Chem Res*. 2010;49:12529–12537.
40. Ha KS, Bae JW, Woo KJ, Jun KW. Efficient utilization of greenhouse gas in a gas-to-liquids process combined with carbon dioxide reforming of methane. *Environ Sci Technol*. 2010;44:1412–1417.
41. Heimel S, Lowe C. Technology comparison of CO_2 capture for a gas-to-liquids plant. *Energy Procedia*. 2009;1:4039–4046.
42. Bin C, Hingguang J, Lin G. System study on natural gas-based polygeneration system of DME and electricity. *Int J Energy Res*. 2008;32:722–734.
43. Hall KR. A new gas to liquids (GTL) or gas to ethylene (GTE) technology. *Catal Today*. 2005;106:243–246.
44. Suzuki S, Sasaki T, Kojima T. New process development of natural gas conversion technology to liquid fuels via OCM reaction. *Energy Fuels*. 1996;10:531–536.
45. Horstman D, Abata D, Keith J, Oberto L. Feasibility study of an onboard natural gas to dimethyl ether reactor for dimethyl ether preinjection and enjanced ignition. *J Eng Gas Turbines Power*. 2005;127:909–917.
46. Erturk, M. Economic analysis of unconventional liquid fuel sources. *Renew Sustain Energy Rev*. 2011;15:2766–2771.
47. Vliet O, Faaij A, Turkenburg W. Fischer–Tropsch diesel production in a well-wheel perspective: a carbon, energy flow and cost analysis. *Energy Convers Manage*. 2009;50(4):855–876.
48. Martin M, Grossmann IE. Process optimization of FT-diesel production from lignocellulosic switchgrass. *Ind Eng Chem Res*. 2011;50:13485–13499.
49. Ellepola J, Thijssen N, Grievink J, Baak G, Avhale A, vanSchijndel J. Development of a synthesis tool for gas-to-liquid complexes. *Comp Chem Eng*. 2012;42:2–14.
50. Duran MA, Grossmann IE. Simultaneous optimization and heat integration of chemical processes. *AIChE J*. 1986;32(1):123–138.
51. Karuppiah R, Grossmann IE. Global optimization for the synthesis of integrated water systems in chemical processes. *Comp Chem Eng*. 2006;30(4):650–673.
52. Ahmetovic E, Grossmann IE. Optimization of energy and water consumption in corn-based ethanol plants. *Ind Eng Chem Res*. 2010;49(17):7972–7982.
53. Grossmann IE, Martín M. Energy and water optimization in biofuel plants. *Chin J Chem Eng*. 2010;18(6):914–922.
54. Ahmetovic E, Grossmann IE. Global superstructure optimization for the design of integrated process water networks. *AIChE J*. 2010;57(2):434–457.
55. National Energy Technology Laboratory. Quality Guidelines for Energy System Studies. National Energy Technology Laboratory, 2004.
56. National Energy Technology Laboratory. Assessment of Hydrogen Production with CO_2 Capture Volume 1: Baseline State-of-the-Art Plants. Document Number: DOE/NETL-2010/1434, 2010.
57. Zhang Q, He D, Li J, Xu B, Liang Y, Zhu Q. Comparatively high yield methanol production from gas phase partial oxidation of methane. *Appl Catal A*. 2002;224:201–207.
58. Zhang Q, He D, Zhu Q. Recent progress in direct partial oxidation of methane to methanol. *J Nat Gas Chem*. 2003;12:81–89.
59. Rasmussen CL, Glarborg P. Direct partial oxidation of natural gas to liquid chemicals: chemical kinetic modeling and global optimization. *Ind Eng Chem Res*. 2008;47(17):6579–6588.
60. Keller GE, Bhasin MM. Synthesis of ethylene via oxidative coupling of methane. I. Determination of active catalysts. *J Catal*. 1992;73(1):9–19.
61. Jones AC, Leonard JJ, Sofranko JA. The oxidative conversion of methane to higher hydrocarbons over alkali-promoted Mn/SiO_2. *J Catal*. 1987;103:311–319.
62. Lee JS, Oyama ST. Oxidative coupling of methane to higher hydrocarbons. *Catal Rev—Sci Eng*. 1988;30(2):249–280.
63. Jones AC, Leonard JJ, Sofranko JA. The oxidative conversion of methane to higher hydrocarbons over alkali-promoted Mn/SiO_2. U.S. Patents 4,443,644, 4,443,645, 4,443,646, 4,443,647, 4,443,648, 4,443,649, 4,444,984 (1984); 4,448,322, 4,499,323, 4,523,049, 4,523,050, 4,544,784, 4,560,821 (1985); 4,567,307 (1986).
64. Fox JM III, Chen TP, Degen BD. An evaluation of direct methane conversion processes. *Chem Eng Prog*. 1990;86:42–50.
65. Lunsford JH. The catalytic oxidative coupling of methane. *Agnew Chem Int Ed Engl*. 1995;34:970–980.
66. Hall KR, Holtzapple MT, Capareda SC. Integrated biofuel production system. U.S. Patent 8,153,850 (2012).
67. Hall KR, Bullin JA, Eubank PT, Akgerman A, Anthony RG. Method for converting natural gas to olefins. U.S. Patents 6,130,260 (2000); 6,323,247 (2001); 6,433,235 (2002); 6,602,920 (2003); 7,045,670, 7,119,240 (2006); 7,183,451, 7,208,647, 7,250,449 (2007); 7,408,091 (2008).
68. Mobil Research and Development Corporation. Slurry Fischer–Tropsch/Mobil Two Stage Process of Converting Syngas to High Octane Gasoline. USDOE contract DE-AC22-80PC30022, 1983.
69. Mobil Research and Development Corporation. Two-Stage Process for Conversion of Synthesis Gas to High Quality Transporation Fuels. USDOE contract DE-AC22-83PC60019, 1985.
70. Bechtel. Aspen Process Flowsheet Simulation Model of a Battelle Biomass-Based Gasification, Fischer–Tropsch Liquefaction and Combined-Cycle Power Plant. Contract Number: DE-AC22-93PC91029, 1998. Available at: http://www.fischer-tropsch.org/. Accessed Aug. 2012.
71. Bechtel. Baseline design/economics for advanced Fischer–Tropsch technology. Contract No. DE-AC22-91PC90027, 1992.
72. National Renewable Energy Laboratory. Gasoline from Wood via Integrated Gasification, Synthesis, and Methanol-to-Gasoline Technologies. USDOE contract DE-AC36-08GO28308, 2011.
73. Mobil Research and Development Corporation. Research Guidance Studies to Assess Gasoline from Coal by Methanol-To-Gasoline and Sasol-Type Fischer–Tropsch Technologies. USDOE contract EF-77-C-O1-2447, 1978.
74. Tabak SA, Yurchak S. Conversion of methanol over ZSM-5 to fuels and chemicals. *Catal Today*. 1990;6(3):307–327.
75. National Energy Technology Laboratory. Cost and Performance Baseline for Fossil Energy Plants. Vol. 1: Bituminous Coal and Natural Gas to Electricity Final Report. Document Number: DOE/NETL-2007/1281, 2007. Available at: http://www.netl.doe.gov/energy-analyses/baseline_studies.html. Accessed Aug. 2012.
76. Chemical Engineering Magazine. Chemical Engineering Plant Cost Index, 2012. Available at: http://www.che.com/pci/ Accessed Aug. 2012.
77. CPLEX. ILOG CPLEX C++ API 12.1 Reference Manual, IBM Corporation, 2009.
78. Drud A. Conopt: a GRG code for large sparse dynamic nonlinear optimization problems. *Math Program*. 1985;31(2):153–191.
79. Floudas CA. Nonlinear and Mixed-Integer Optimization. New York: Oxford University Press, 1995.
80. Floudas CA. Deterministic Global Optimization: Theory, Methods and Applications. Dordrecht, The Netherlands: Kluwer Academic Publishers, 2000.
81. Floudas CA, Pardalos PM. State of the art in global optimization: computational methods and applications. *J Global Optim*. 1995;7(2):113.
82. Floudas CA, Akrotirianakis IG, Caratzoulas S, Meyer CA, Kallrath J. Global optimization in the 21st century: advances and challenges. *Comp Chem Eng*. 2005;29(6):1185–1202.
83. Floudas CA, Gounaris CE. A review of recent advances in global optimization. *J Global Optim*. 2009;45(1):3–38.
84. Energy Information Administration. Annual Energy Outlook 2011 with Projections to 2035. Document Number: DOE/EIA-0383(2011), 2011. Available at: http://www.eta.doe.gov/oiaf/aeo/. Accessed Aug. 2012.
85. Floudas CA, Ciric AR, Grossmann IE. Automatic synthesis of optimum heat exchanger network configurations. *AIChE J*. 1986;32(2):276–290.
86. Gregor JH, Gosling CD, Fullerton HE. Upgrading Fischer–Tropsch LPG with the Cyclar Process. Contract No. DE-AC22-86PC90014, 1989.
87. Argonne National Laboratory. GREET 1.8b, The Greenhouse Gases, Regulated Emissions, and Energy Use in Transportation (GREET) Model. Argonne National Laboratory, Argonne, IL 2007; Released September 2008.

APPENDIX: A

Mathematical Model for Process Synthesis with Simultaneous Heat, Power, and Water Integration

The nomenclature for all terms in the mathematical model for process synthesis with simultaneous heat, power, and water integration is shown later. All constraints included in the model are listed subsequently with a corresponding description of how that particular equation governs proper operation of the process design. For a more extensive discussion of the mathematical model, the reader is directed to previously published works.[14,15,29,30]

Process Units

The set of units, U, is presented in full detail in Table 3 and defined formally in Eq. A(1). Note that several units in Table A1 are listed as u_n. The n subscript represents the consideration of multiple forms of the same process unit, each with a distinct set of operating conditions (e.g., temperature and pressure). Although these unit properties are generally given as continuous variables in a process synthesis problem, they have been assumed to take discrete choices and will be modeled using binary variables.

$$u \in U = \{\text{Complete set of process units listed in Table A1}\} \quad \text{(A1)}$$

Process Species

The set of all species, S, is listed in Table A2 and defined formally in Eq. A(2).

$$s \in S = \{\text{Complete set of species listed in Table A2}\} \quad \text{(A2)}$$

Indices/Sets

The indices are used throughout the mathematical model are listed as follows.

u = process unit index

s = species index

a = atom index

p = proximate analysis index

r = reaction index

i = general counting index

The set, U, is defined as the complete set of process units. Several subsets of units are then defined for specific areas of the GTL process as presented below.

$$u_{\text{RGS}} = \{u : u = \text{RGS}_n\}$$

$$u_{\text{ATR}} = \{u : u = \text{ATR}_n\}$$

Table A1. Process Units Present in the GTL Synthesis Problem

Unit Name	Unit Index	Unit Name	Unit Index
Process inlets			
Inlet air	IN_{AIR}	Inlet natural gas	IN_{NG}
Inlet water	IN_{H2O}	Inlet Butane	IN_{BUT}
Process outlets			
Outlet gasoline	OUT_{GAS}	Outlet diesel	OUT_{DIE}
Outlet kerosene	OUT_{KER}	Outlet ash	OUT_{ASH}
Outlet sulfur	OUT_{S}	Outlet scrubbed HCl	OUT_{SCR}
Outlet vent	OUT_{V}	Outlet propane	OUT_{PRO}
Outlet sequestered CO_2	OUT_{CO_2}	Outlet wastewater	OUT_{WW}
Natural gas conversion			
Autothermal reactor	ATR	Steam reformer	SMR
Partial oxidation	POM	OC	OCO
OC catalyst regeneration	OCO-CAT	OC water knock out	OCO-F
OC CO_2 removal	OCO-CO_2		
Syngas cleaning			
Reverse water gas shift unit	RGS_n	RGS effluent cooler	X_{RGS}
COS-HCN hydrolyzer	CHH	HCl scrubber	HSC
Acid gas flash vapor cooler	X_{AGF}	Acid gas flash 2-phase cooler	X_{AGF_n}
Acid gas flash unit	AGF	Acid gas thermal analyzer	X_{AGR}
Acid gas removal unit	AGR	First CO_2 compressor	CO_2C
CO_2 recycle compressor	CO_2RC	CO_2 sequestration compressor	CO_2SC
Acid gas compressor	AGC		
Hydrocarbon production			
Iron MT fWGS nominal wax FT	MTFTWGS-N	Iron MT fWGS minimal was FT	MTFTWGS-M
FT compressor	FTC	FT splitter	SP_{FT}
Low-temperature preheater	X_{LTFT}	Low-temperature splitter	SP_{LTFT}
Low-temperature iron-based FT	LTFT	Low-temperature cobalt-based FT	LTFTRGS
High-temperature preheater	X_{HTFT}	High-temperature splitter	SP_{HTFT}
High-temperature iron-based FT	HTFT	High-temperature cobalt-based FT	HTFTRGS
ZSM-5 hydrocarbon conversion unit	FT-ZSM5	ZSM-5 product fractionation	ZSM5F
Methanol synthesis unit	MEOHS	Methanol flash unit	MEOH-F
Methanol degasser	MEDEG	Methanol to gasoline ZSM-5 reactor	MTG
Methanol to olefins ZSM-5 reactor	MTO	MTO fractionation	MTO-F
Low-temperature effluent cooler	X_{LTFTC}	High-temperature effluent cooler	X_{HTFTC}
Water-soluble oxygenates separator	WSOS	Vapor-phase oxygenates separator	VPOS
Primary vapor–liquid–water separator	VLWS		

TABLE A1. *Continued*

Unit Name	Unit Index	Unit Name	Unit Index
Hydrocarbon recovery			
Hydrocarbon recovery column	HRC	Wax hydrocracker	WHC
Distillate hydrotreater	DHT	Kerosene hydrotreater	KHT
Naphtha hydrotreater	NHT	Naphtha reformer	NRF
C_4 isomerizer	C_4I	C_5—C_6 isomerizer	$C_{56}I$
C_3—C_4—C_5 alkylation unit	$C_{345}A$	Saturated gas plant	SGP
Diesel blender	DBL	Gasoline blender	GBL
Olefins to gasoline/distillate	OGD	OGD fractionation	OGD-F
Mixed hydrocarbon knockout 1	HCKO1	Mixed hydrocarbon knockout 2	
De-ethanizer	DEETH	Absorber column	ABS-COL
1-stage Rectisol CO_2 separation	CO_2SEP	Stabilizer column	
HF alkylation unit	ALK-UN	LPG/alkylate splitter	LPG-ALK
Splitter column	SP-COL		
Recycle gas treatment			
Light gas compressor	LGC	Light gas splitter	SP_{LG}
Fuel combustor	FCM	Fuel combuster effluent cooler	X_{FCM}
Fuel combustor flash unit	FCF	First GT air compressor	$GTAC_1$
Second GT air compressor	$GTAC_2$	GT combustor	GTC
First GT	GT_1	Second GT	GT_2
GT effluent cooler	X_{GT}	GT flash unit	GTF
GT effluent compressor	GTEC	CO_2 recovery unit	CO_2R
Water gas shift unit	WGS		
Water treatment			
Biological digestor	BD	Reverse osmosis	RO
Cooling tower	CLTR	Process cooling	COOL-P
Heat and power system	HEP	Heat and power utilities	HEAT-P
Deaerator	DEA	Process water economizer	X_{WPR}
Process water boiler	X_{WBL}		
Hydrogen/oxygen production			
PSA effluent splitter	SP_{PSA}	Pressure-swing adsorption unit	PSA
PSA hydrogen preheater	X_{H_2P}	PSA hydrogen splitter	SP_{H_2P}
Electrolyzer	EYZ	Electrolyzer oxygen preheater	X_{O_2E}
Electrolyzer oxygen splitter	SP_{O_2E}	Electrolyzer hydrogen preheater	X_{H_2E}
Electrolyzer hydrogen splitter	SP_{H_2E}	Air compressor	AC
Air separation unit	ASU	Oxygen compressor	OC
ASU oxygen preheater	X_{O_2A}	OC oxygen splitter	SP_{O_2C}
OC oxygen preheater	X_{O_2C}		

The subscript n corresponds to multiple forms of the same process unit, each with a distinct set of operating conditions or ratios of feedstock. Distinct process units are used *in lieu* of continuous variables representing the process operating conditions. This will prevent the use of bilinear terms when specifying feedstock ratios or highly nonlinear equations when specifying equilibrium constants or species enthalpies.

The set of all atoms, A, includes C, H, O, N, S, Cl, and Ar.

$$a \in A = \{\mathrm{C},\ \mathrm{H},\ \mathrm{O},\ \mathrm{N},\ \mathrm{S},\ \mathrm{Cl},\ \mathrm{Ar}\}$$

The list of all unit connections, UC, is derived as follows.

$$\mathrm{UC} = \{(u,u') : \exists \text{ a connection between unit } u \text{ and unit } u' \text{ in the superstructure}\}$$

Using *a priori* knowledge about the operations of each unit in the GTL process, the complete set of species that can possibly exist in a stream from unit u to unit u' is defined as $S^{\mathrm{UC}}_{u,u'}$. The set $(u,u',s) \in S^{\mathrm{UF}}$ is then constructed from all streams in UC along with the set of all species s that exist within a given unit u (S^U).

$$S^{\mathrm{UF}} = \{(u,u',s) : \exists s \in S^{\mathrm{UC}}_{u,u'}\}$$

$$S^U = \{(s,u) : \exists (u,u',s) \in S^{\mathrm{UF}} \text{ or } \exists (u',u,s) \in S^{\mathrm{UF}}\}$$

Parameters

With the exception of all the pseudocomponents, the molecular formula is equal to the species index defined in Table A2. The pseudocomponent hydrocarbons and oxygenate formulas are given by Bechtel while the formulas for biomass and coal compounds are derived from the ultimate analysis and normalized to one mole of carbon. Char has been assumed to consist completely of carbon and ash has been assigned a generic molecular weight of 1.0 g/mol. The atomic ratio ($\mathrm{AR}_{s,a}$) of atom a in species s is derived from the molecular formulas in Table A2.

$$\mathrm{AR}_{s,a} = \text{atomic ratio of atom } a \text{ in species } s$$

Using the appropriate atomic weight of atom a (AW_a), the molecular weight of all species s (MW_s) is defined using Eq. A(3).

$$\mathrm{AW}_a = \text{atomic weight of atom } a$$
$$\mathrm{MW}_s = \sum\nolimits_a \mathrm{AW}_a \cdot \mathrm{AR}_{s,a} \tag{A3}$$

Variables

Continuous variables are used in the mathematical model to describe the species molar flow rates ($N^{\mathrm{S}}_{u,u',s}$), the total molar flow rates ($N^{\mathrm{T}}_{u,u'}$), the extent of reaction in a process unit (ξ^u_r), the molar composition of a stream ($x^{\mathrm{S}}_{u,u',s}$), the split fraction of a stream between two units ($\mathrm{sp}_{u,u'}$), the total stream enthalpy flow rate ($H^{\mathrm{T}}_{u,u'}$), the heat lost from a unit

Table A2. Species Present in the GTL Synthesis Problem

Species Name	Species Index	Species Name	Species Index	Species Name	Species Index
Light nonhydrocarbon gases					
Oxygen	O_2	Nitrogen	N_2	Argon	Ar
Nitric oxide	NO	Nitrous oxide	N_2O	Water	H_2O
Carbon monoxide	CO	Hydrogen	H_2	Carbon dioxide	CO_2
Hydrocarbons					
Methane	CH_4	Acetylene	C_2H_2	Ethylene	C_2H_4
Ethane	C_2H_6	Propylene	C_3H_6	Propane	C_3H_8
Isobutylene	iC_4H_8	1-Butene	nC_4H_8	Isobutane	iC_4H_{10}
n-Butane	nC_4H_{10}	1-Pentene	C_5H_{10}	2-Methylbutane	iC_5H_{12}
n-Pentane	nC_5H_{12}	1-Hexene	C_6H_{12}	2-Methylpentane	iC_6H_{14}
n-Hexane	nC_6H_{14}	1-Heptene	C_7H_{14}	*n*-Heptane	C_7H_{16}
1-Octene	C_8H_{16}	n-Octane	C_8H_{18}	1-Nonene	C_9H_{18}
n-Nonane	C_9H_{20}	1-Decene	$C_{10}H_{20}$	*n*-Decane	$C_{10}H_{22}$
1-Undecene	$C_{11}H_{22}$	*n*-Undecane	$C_{11}H_{24}$	1-Dodecene	$C_{12}H_{24}$
n-Dodecane	$C_{12}H_{26}$	1-Tridecene	$C_{13}H_{26}$	*n*-Tridecane	$C_{13}H_{28}$
1-Tetradecene	$C_{14}H_{28}$	*n*-Tetradecane	$C_{14}H_{30}$	1-Pentadecene	$C_{15}H_{30}$
n-Pentadecane	$C_{15}H_{32}$	1-Hexadecene	$C_{16}H_{32}$	*n*-Hexadecane	$C_{16}H_{34}$
1-Heptadecene	$C_{17}H_{34}$	*n*-Heptadecane	$C_{17}H_{36}$	1-Octadecene	$C_{18}H_{36}$
n-Octadecane	$C_{18}H_{38}$	1-Nonadecene	$C_{19}H_{38}$	*n*-Nonadecane	$C_{19}H_{40}$
1-Eicosene	$C_{20}H_{40}$	*n*-Eicosane	$C_{20}H_{42}$	C_{21} pseudocomponent	$C_{21}OP$
C_{22} pseudocomponent	$C_{22}OP$	C_{23} pseudocomponent	$C_{23}OP$	C_{24} pseudocomponent	$C_{24}OP$
C_{25} pseudocomponent	$C_{25}OP$	C_{26} pseudocomponent	$C_{26}OP$	C_{27} pseudocomponent	$C_{27}OP$
C_{28} pseudocomponent	$C_{28}OP$	C_{29} pseudocomponent	$C_{29}OP$	C_{30+} pseudocomponent	C_{30} wax
VP oxygenate	OXVAP	HP oxygenate	OXHC	AP oxygenate	OXH2O
Methanol	CH_3OH				
Products					
Gasoline	GAS	Diesel	DIE	Kerosene	KER
LPG	LPG				

The molecular formula of the pseudocomponent hydrocarbons and oxygenates are given by Bechtel. The formula for the biomass and coal species are derived from the ultimate analysis assuming that the "atomic" weight of ash is 1.0 g/mol.

(Q_u^{L}), the heat transferred to or absorbed from a unit (Q_u), the delivered cost of feedstock ($\mathrm{Cost}_s^{\mathrm{F}}$), the cost of CO_2 sequestration ($\mathrm{Cost}^{\mathrm{Seq}}$), the cost of electricity ($\mathrm{Cost}^{\mathrm{El}}$), and the levelized unit investment cost (Cost_u^U). Note that the subscripts u and u' are both used to denote an element of the set U and can be used interchangeably in the stream flow indices.

$N_{u,u',s}^{\mathrm{S}}$ = molar flow of species s from unit u to unit u'

$N_{u,u'}^{\mathrm{T}}$ = total molar flow from unit u to unit u'

ξ_r^u = extent of reaction r in unit u

$x_{u,u',s}^{\mathrm{S}}$ = molar composition of species s from u to unit u'

$\mathrm{sp}_{u,u'}$ = split fraction of stream going from unit u to unit u'

$H_{u,u'}^{\mathrm{T}}$ = total enthalpy flow from unit u to unit u'

Q_u^{L} = heat lost from unit u

Q_u = heat transferred to or absorbed from from unit u

$\mathrm{Cost}_s^{\mathrm{F}}$ = total delivered cost of feedstock$s$

$\mathrm{Cost}^{\mathrm{Seq}}$ = total sequestration cost of CO_2

$\mathrm{Cost}^{\mathrm{El}}$ = total cost of electricity

Cost_u^U = total levelized cost of unit u

Binary variables (y_u) are introduced to represent the logical use of a process unit u. These binary variables are only needed for specific process, because many of the units in the GTL process will always be required. The units that require binary variables include the reverse water gas shift unit, the FT units, the autothermal reformer, the steam reformer, the gas turbine, the methanol synthesis unit, the methanol conversion units, and each of the hydrocarbon upgrading units.

y_u = logical existence of process unit u(i.e., it takes the value of one if unit u is selected and zero otherwise)

General Constraints

Material balances

Species Balances.

$$\sum_{(u',u)\in \mathrm{UC}} N_{u',u,s}^{\mathrm{S}} - \sum_{(u,r,s')\in R^U} \frac{\nu_{r,s}}{\nu_{r,s'}} \cdot \xi_r^u - \sum_{(u,u')\in \mathrm{UC}} N_{u,u',s}^{\mathrm{S}} = 0 \qquad \forall s \in S_u^U, u \in U_{\mathrm{Sp}}^{\mathrm{Bal}} \tag{A4}$$

Extent of Reaction.

$$\xi_r^u - \mathrm{fc}_r^u \cdot \sum_{(u',u,s)\in S^{\mathrm{UF}}} N_{u',u,s}^{\mathrm{S}} = 0 \qquad \forall (u,r,s) \in R^U \tag{A5}$$

Atom Balances.

$$\sum_{(u',u,s)\in S^{\mathrm{UF}}} \mathrm{AR}_{s,a} \cdot N_{u',u,s}^{\mathrm{S}} - \sum_{(u,u',s)\in S^{\mathrm{UF}}} \mathrm{AR}_{s,a} \cdot N_{u,u',s}^{\mathrm{S}} = 0 \qquad \forall a \in A_u^U, u \in U_{\mathrm{At}}^{\mathrm{Bal}} \tag{A6}$$

Total Mole Balance.

$$N_{u',u}^{\mathrm{T}} - \sum_{(u,u',s)\in S^{\mathrm{UF}}} N_{u',u,s}^{\mathrm{S}} = 0 \qquad \forall (u,u') \in \mathrm{UC} \tag{A7}$$

Process splitters

Set Unit Split Fractions.

$$N_{u,u',s}^{\mathrm{S}} - x_{u_l,u,s}^{\mathrm{S}} \cdot N_{u,u'}^{\mathrm{T}} = 0 \qquad \forall (u,u',s) \in S^{\mathrm{UF}}, \quad u \in U_{\mathrm{Sp}} \tag{A8}$$

Split Fractions Sum to 1.

$$\sum_{(u,u',s)\in S^{\mathrm{UF}}} x^{\mathrm{S}}_{u,u',s} - 1 = 0 \qquad \forall (u,u') \in \mathrm{UC}_{\mathrm{Comp}} \tag{A9}$$

Flash units

Upper Bound of Liquid Phase Split Fraction.

$$x^{\mathrm{S}}_{u,u_{\mathrm{L}},s} - \min\left\{1, \frac{1}{K^{\mathrm{VLE}}_{u,s}}\right\} \le 0 \qquad \forall (u,u_{\mathrm{L}},s) \in S^{\mathrm{UF}}, \qquad u \in U_{\mathrm{Fl}} \tag{A10}$$

Upper Bound of Vapor Phase Split Fraction.

$$x^{\mathrm{S}}_{u,u_{\mathrm{V}},s} - \min\{1, K^{\mathrm{VLE}}_{u,s}\} \le 0 \qquad \forall (u,u_{\mathrm{V}},s) \in S^{\mathrm{UF}}, \qquad u \in U_{\mathrm{Fl}} \tag{A11}$$

Set Liquid Phase Split Fraction.

$$x^{\mathrm{S}}_{u,u_{\mathrm{L}},s} \cdot N^{\mathrm{T}}_{u,u_{\mathrm{L}}} - N^{\mathrm{S}}_{u,u_{\mathrm{L}},s} = 0 \qquad \forall u \in U_{\mathrm{Fl}} \tag{A12}$$

Set Vapor Phase Split Fraction.

$$x^{\mathrm{S}}_{u,u_{\mathrm{V}},s} \cdot N^{\mathrm{T}}_{u,u_{\mathrm{V}}} - N^{\mathrm{S}}_{u,u_{\mathrm{V}},s} = 0 \qquad \forall u \in U_{\mathrm{Fl}} \tag{A13}$$

Set Phase Equilibrium.

$$x^{\mathrm{S}}_{u,u_{\mathrm{V}},s} - K^{\mathrm{VLE}}_{u,s} \cdot x^{\mathrm{S}}_{u,u_{\mathrm{L}},s} = 0 \qquad \forall u \in U_{\mathrm{Fl}} \tag{A14}$$

Heat balances

Conservation of Energy.

$$\sum_{(u,u')\in \mathrm{UC}} H^{\mathrm{T}}_{u,u'} - \sum_{(u',u)\in \mathrm{UC}} H^{\mathrm{T}}_{u',u} - Q_u - Q^{\mathrm{L}}_u - W_u = 0 \qquad \forall u \in U/U_{\mathrm{Agg}} \tag{A15}$$

Total Heat Balance.

$$H^{\mathrm{T}}_{u,u'} - \sum_{(u,u',s)\in S^{\mathrm{UF}}} H^{\mathrm{S}}_{u,u',s} = 0 \qquad \forall (u,u') \in \mathrm{UC} \tag{A16}$$

Logical unit existence

Bound on Molar Flows.

$$\sum_{(u',u)\in \mathrm{UC}} N^{\mathrm{T}}_{u',u} - UB^{\mathrm{N}}_u \cdot y_u \le 0 \qquad \forall u \in U^{\mathrm{Ex}} \tag{A17}$$

Upper Bound on Inlet Enthalpy Flow.

$$H^{\mathrm{T}}_{u',u} - \mathrm{UB}^{\mathrm{H}}_{u',u} \cdot y_u \le 0 \qquad \forall (u',u) \in \mathrm{UC}, \qquad u \in U^{\mathrm{Ex}} \tag{A18}$$

Lower Bound on Inlet Enthalpy Flow.

$$\mathrm{LB}^{\mathrm{H}}_{u',u} \cdot y_u - H^{\mathrm{T}}_{u',u} \le 0 \qquad \forall (u',u) \in \mathrm{UC}, \qquad u \in U^{\mathrm{Ex}} \tag{A19}$$

Upper Bound on Outlet Enthalpy Flow.

$$H^{\mathrm{T}}_{u,u'} - \mathrm{UB}^{\mathrm{H}}_{u',u} \cdot y_u \le 0 \qquad \forall (u,u') \in \mathrm{UC}, \qquad u \in U^{\mathrm{Ex}} \tag{A20}$$

Lower Bound on Outlet Enthalpy Flow.

$$\mathrm{LB}^{\mathrm{H}}_{u,u'} \cdot y_u - H^{\mathrm{T}}_{u,u'} \le 0 \qquad \forall (u,u') \in \mathrm{UC}, \qquad u \in U^{\mathrm{Ex}} \tag{A21}$$

Process Inlets

Known stream compositions

Set Stream Compositions for Inlet Streams.

$$N^{\mathrm{S}}_{u,u',s} - x^{\mathrm{K}}_{u,s} \cdot N^{\mathrm{T}}_{u,u'} = 0 \qquad \forall (u,u',s) \in S^{\mathrm{UF}}, \qquad u = \{\mathrm{IN}_{\mathrm{AIR}}, \mathrm{IN}_{\mathrm{NG}}, \mathrm{IN}_{\mathrm{BUT}}\} \tag{A22}$$

Greenhouse gas emissions reduction

Set Reduction from Petroleum Based Processes.

$$\mathrm{GHG}_{\mathrm{GTL}} - \mathrm{GHG}_{\mathrm{Red}} \cdot (\mathrm{GHG}_{\mathrm{Pet}} + \mathrm{GHG}_{\mathrm{Elec}}) = 0 \tag{A23}$$

Sum Emissions from GTL Components.

$$\mathrm{GHG}_{\mathrm{GTL}} - \mathrm{GHG}^{\mathrm{Seq}} - \mathrm{GHG}^{\mathrm{Proc}} - \mathrm{GHG}^{\mathrm{Feed}} = 0 \tag{A24}$$

Set Emissions from Feedstock Acquisition.

$$\mathrm{GHG}^{\mathrm{Feed}} - \sum_{u\in U_{\mathrm{In}}} \sum_{(u,u',s)\in S^{\mathrm{UF}}} \mathrm{GHG}^{\mathrm{T}}_s \cdot \mathrm{MW}_s \cdot N^{\mathrm{S}}_{u,u',s} = 0 \tag{A25}$$

Set Emissions from CO_2 Sequestration.

$$\mathrm{GHG}^{\mathrm{Seq}} - \mathrm{GHG}^{\mathrm{T}}_{\mathrm{CO_2}} \cdot \mathrm{MW}_{\mathrm{CO_2}} \cdot N^{\mathrm{S}}_{\mathrm{CO_2SC,OUT_{CO_2},CO_2}} = 0 \tag{A26}$$

Set Emissions from CO_2 Venting.

$$\mathrm{GHG}^{\mathrm{Proc}} - \mathrm{MW}_{\mathrm{CO_2}} \cdot N^{\mathrm{S}}_{\mathrm{CO_2R,OUT_V,CO_2}} = 0 \tag{A27}$$

Process Outlet Fuel Ratios

Set gasoline to diesel output ratio

$$\mathrm{MW}_{\mathrm{GAS}} \cdot N^{\mathrm{S}}_{\mathrm{GBL,OUT_{GAS},GAS}} - \mathrm{Rat}_{\mathrm{G\text{-}D}} \cdot \mathrm{MW}_{\mathrm{DIE}} \cdot N^{\mathrm{S}}_{\mathrm{DBL,OUT_{DIE},DIE}} = 0 \tag{A28}$$

Set diesel to kerosene output ratio

$$\mathrm{MW}_{\mathrm{DIE}} \cdot N^{\mathrm{S}}_{\mathrm{DBL,OUT_{DIE}}}, \mathrm{DIE} - \mathrm{Rat}_{\mathrm{D\text{-}K}} \cdot \mathrm{MW}_{\mathrm{KER}} \cdot N^{\mathrm{S}}_{\mathrm{KHT,OUT_{KER},KER}} = 0 \tag{A29}$$

Natural Gas Conversion

Autothermal reactor

Logical Use of One Temperature.

$$\sum_{u\in U_{\mathrm{ATR}}} y_u - 1 = 0 \tag{A30}$$

Water-Gas-Shift Equilibrium.

$$N^{\mathrm{S}}_{u,u',\mathrm{CO_2}} \cdot N^{\mathrm{S}}_{u,u',\mathrm{H_2}} - K^{\mathrm{RGS}}_u \cdot N^{\mathrm{S}}_{u,u',\mathrm{CO}} \cdot N^{\mathrm{S}}_{u,u',\mathrm{H_2O}} = 0 \qquad \forall (u,u') \in \mathrm{UC}, \qquad u \in U_{\mathrm{ATR}} \tag{A31}$$

CH_4 Steam Reforming Equilibrium.

$$x^{S}_{u,u',CO} \cdot x^{S}_{u,u',H_2}{}^{3} - K^{SR}_{u,CH_4} \cdot x^{S}_{u,u',CH_4} \cdot x^{S}_{u,u',H_2O} = 0 \quad \forall (u,u') \in UC, \quad u \in U_{ATR} \tag{A32}$$

Bypass of Inert Species.

$$\sum_{(u',u,s)\in S^{UF}} N^{S}_{u',u,s} - \sum_{(u,u',s)\in S^{UF}} N^{S}_{u,u',s} = 0 \quad \forall u \in U_{ATR}, \quad s \in S^{In}_{ATR} \tag{A33}$$

Steam reformer

Logical Use of One Temperature.

$$\sum_{u\in U_{SMR}} y_u - 1 = 0 \tag{A34}$$

Water-Gas-Shift Equilibrium.

$$N^{S}_{u,u',CO_2} \cdot N^{S}_{u,u',H_2} - K^{RGS}_{u} \cdot N^{S}_{u,u',CO} \cdot N^{S}_{u,u',H_2O} = 0 \quad \forall (u,u') \in UC, \quad u \in U_{SMR} \tag{A35}$$

CH_4 Steam Reforming Equilibrium.

$$x^{S}_{u,u',CO} \cdot x^{S}_{u,u',H_2}{}^{3} - K^{SR}_{u,CH_4} \cdot x^{S}_{u,u',CH_4} \cdot x^{S}_{u,u',H_2O} = 0 \quad \forall (u,u') \in UC, \quad u \in U_{SMR} \tag{A36}$$

Bypass of Inert Species.

$$\sum_{(u',u,s)\in S^{UF}} N^{S}_{u',u,s} - \sum_{(u,u',s)\in S^{UF}} N^{S}_{u,u',s} = 0 \quad \forall u \in U_{SMR}, \quad s \in S^{In}_{SMR} \tag{A37}$$

Partial oxidation to methanol

Conversion of Methane.

$$N^{S}_{POM,u,CH_4} = fc_{POM,CH_4} \cdot \sum_{(u',POM,CH_4)\in S^{UF}} N^{S}_{u',POM,CH_4} \tag{A38}$$

Selectivity to Products.

$$N^{S}_{POM,u,s} \cdot AR_{s,C} = cd_{POM,CH_4} \cdot \sum_{(u',POM,CH_4)\in S^{UF}} N^{S}_{u',POM,CH_4} \quad \forall s \in S^{Ef}_{POM} \tag{A39}$$

Oxidative coupling to olefins

Conversion of Alkanes.

$$N^{S}_{OCO,u,s} = fc_{OCO,s} \cdot \sum_{(u',OCO,s)\in S^{UF}} N^{S}_{u',OCO,s} \quad \forall s \in S^{HC}_{OCO} \tag{A40}$$

Selectivity to Products.

$$N^{S}_{OCO,u,s} \cdot AR_{s,C} = cd_{OCO,s} \cdot \sum_{s\in S^{HC}_{OCO}} \sum_{(u',OCO,s)\in S^{UF}} N^{S}_{u',OCO,s} \quad \forall s \in S^{Ef}_{OCO} \tag{A41}$$

Hydrocarbon Production

FT

Set Ratio of H_2 to CO in Cobalt-Based Inlet.

$$\sum_{(u',u,H_2)\in S^{UF}} -FTR_{u,H_2} \cdot \sum_{(u',u,CO)\in S^{UF}} -FTR_{u,CO} = 0 \quad \forall u \in U_{CoFT} \tag{A42}$$

Set Ratio of H_2 to CO and CO_2 in Iron-Based Inlet.

$$\sum_{(u',u,H_2)\in S^{UF}} -FTR_{u,H_2} \cdot \sum_{(u',u,CO)\in S^{UF}} -FTR_{u,CO} \cdot \sum_{(u',u,CO_2)\in S^{UF}} -FTR_{u,CO_2} = 0 \quad \forall u \in U_{IrFT} \tag{A43}$$

Adjust Weight Fraction of C_1 Species.

$$W_1 = \frac{1}{2}\left(1 - \sum_{n=5}^{\infty} W_n\right) \tag{A44}$$

Adjust Weight Fraction of C_2 Species.

$$W_2 = \frac{1}{6}\left(1 - \sum_{n=5}^{\infty} W_n\right) \tag{A45}$$

Adjust Weight Fraction of C_3 Species.

$$W_3 = \frac{1}{6}\left(1 - \sum_{n=5}^{\infty} W_n\right) \tag{A46}$$

Adjust Weight Fraction of C_4 Species.

$$W_4 = \frac{1}{6}\left(1 - \sum_{n=5}^{\infty} W_n\right) \tag{A47}$$

Set Weight Fraction of C_n Species from Anderson–Schultz–Flory Distribution.

$$W_n = n(1-\alpha)^2\alpha^{n-1} \quad \forall 5 \le n \le 29 \tag{A48}$$

Set Weight Fraction of Wax.

$$W_{Wax} = \sum_{n=30}^{\infty} n(1-\alpha)^2\alpha^{n-1} \tag{A49}$$

Set Carbon Distribution from Weight Fractions.

$$cr_n = \frac{n \cdot W_n}{\sum_{n=1}^{29} n \cdot W_n + n_{Wax} \cdot W_{Wax}} \tag{A50}$$

Set Exactly One Low-Temperature Unit.

$$y_{LTFT} + y_{LTFTRGS} - 1 = 0 \tag{A51}$$

Set Exactly One High-Temperature Unit.

$$y_{HTFT} + y_{HTFTRGS} - 1 = 0 \tag{A52}$$

Aqueous phase oxygenates separator

Removal of Aqueous Phase Oxygenates.

$$N^{S}_{WSOS,VLWS,s} = 0 \quad \forall s \in S_{APO} \tag{A53}$$

Vapor phase oxygenates separator

Removal of Vapor Phase Oxygenates.

$$N^{S}_{VPOS,HRC,s} = 0 \quad \forall s \in S_{VPO} \tag{A54}$$

Hydrocarbon Upgrading

Hydrocarbon upgrading units

Set Carbon Distribution Fractions of Total Input.

$$N^{\mathrm{S}}_{u,u',s} \cdot \mathrm{AR}_{s,\mathrm{C}} - \mathrm{cf}_{u,u',s} \cdot \sum_{(u'',u,s')\in S^{\mathrm{UF}}} N^{\mathrm{S}}_{u'',u,s'} \cdot \mathrm{AR}_{s',\mathrm{C}} = 0 \quad \forall u \in U_{\mathrm{UG}}, \quad (u,u',s) \in s^{\mathrm{UF}} \tag{A55}$$

Saturated gas plant

Set Fractional Recovery of Light Gases.

$$N^{\mathrm{S}}_{\mathrm{SGP},\mathrm{C_4I},s} - \mathrm{rf}_s \cdot \sum_{(u,\mathrm{SGP},s)\in S^{\mathrm{UF}}} N^{\mathrm{S}}_{u,\mathrm{SGP},s} = 0 \quad \forall s \in S_{\mathrm{C_4}} \tag{A56}$$

Recycle Gas Treatment

Fuel combustor

Set Inlet Combustor Oxygen Level.

$$\sum_{(u,\mathrm{FCM})\in \mathrm{UC}} N^{\mathrm{S}}_{u,\mathrm{FCM},\mathrm{O_2}} - \mathrm{er}_{\mathrm{FCM}} \cdot \sum_{(\mathrm{SP_{LG}},\mathrm{FCM},s)\in S^{\mathrm{UF}}} N^{\mathrm{S}}_{\mathrm{SP_{LG}},\mathrm{FCM},s} \cdot \mathrm{sor}_s = 0 \tag{A57}$$

Gas turbine

Set Air Leakage From First Compressor.

$$N^{\mathrm{S}}_{\mathrm{GTAC_1},\mathrm{OUT_V},s} - \mathrm{lk}_{\mathrm{GTAC_1}} \cdot N^{\mathrm{S}}_{\mathrm{IN_{AIR}},\mathrm{GTAC}_{1,s=0}} \quad \forall(\mathrm{GTAC}_{1,s}) \in S^U \tag{A58}$$

Set Air Bypass From First Compressor.

$$N^{\mathrm{S}}_{\mathrm{GTAC_1},\mathrm{GT_2},s} - \mathrm{by}_{\mathrm{GTAC_1}} \cdot N^{\mathrm{S}}_{\mathrm{IN_{AIR}},\mathrm{GTAC}_{1,s=0}} \quad \forall(\mathrm{GTAC}_{1,s}) \in S^U \tag{A59}$$

Set Inlet Oxygen Flow Rate in Combustor.

$$\mathrm{er}_{\mathrm{GTC}} \cdot \sum_{(u,\mathrm{GTC},s)\in S^{\mathrm{UF}}} \mathrm{sor}_s \cdot N^{\mathrm{S}}_{u,\mathrm{GTC},s} - \sum_{(u,\mathrm{GTC},s)\in S^{\mathrm{UF}}} N^{\mathrm{S}}_{u,\mathrm{GTC},\mathrm{O_2}} = 0 \tag{A60}$$

Set Heat Loss in Combustor.

$$Q^{\mathrm{L}}_{\mathrm{GTC}} - \mathrm{hl}_{\mathrm{GTC}} \cdot (H^{\mathrm{T}}_{\mathrm{SP_{LG}},\mathrm{GTC}} - H^{\mathrm{T}}_{\mathrm{X_{GTF}},\mathrm{GTF}}) = 0 \tag{A61}$$

Wastewater Treatment

Biological digestor

Set Biogas Ratio of CH_4 to CO_2.

$$N^{\mathrm{S}}_{\mathrm{BD},\mathrm{CC},\mathrm{CH_4}} - \mathrm{cr}_{\mathrm{BD}} \cdot N^{\mathrm{S}}_{\mathrm{BD},\mathrm{CC},\mathrm{CO_2}} = 0 \tag{A62}$$

Reverse osmosis

Set Removal Fraction of Solids.

$$N^{\mathrm{S}}_{\mathrm{RO},\mathrm{SP_{RO}}}, s - \mathrm{rf}_{\mathrm{RO}} \cdot N^{\mathrm{S}}_{\mathrm{MX_{RO}},\mathrm{RO},s} = 0 \quad \forall s \in S_{\mathrm{Sol}} \tag{A63}$$

Cooling cycle

Cooling Tower Flow Rate from Energy Requirement.

$$Q_{\mathrm{C}} - \mathrm{hr}_{\mathrm{COOL\text{-}P}} \cdot N^{\mathrm{S}}_{\mathrm{CLTR},\mathrm{COOL\text{-}P},\mathrm{H_2O}} = 0 \tag{A64}$$

Cooling Tower Evaporation Loss.

$$N^{\mathrm{Evap}}_{\mathrm{CLTR}} - 0.00085 \cdot \Delta T_{\mathrm{CLTR}} \cdot N^{\mathrm{S}}_{\mathrm{CLTR},\mathrm{COOL\text{-}P},\mathrm{H_2O}} = 0 \tag{A65}$$

Cooling Tower Drift Loss.

$$N^{\mathrm{Drift}}_{\mathrm{CLTR}} - 0.001 \cdot N^{\mathrm{S}}_{\mathrm{MX_{CLTR}},\mathrm{CLTR},\mathrm{H_2O}} = 0 \tag{A66}$$

Sum Total Cooling Tower Losses.

$$N^{\mathrm{Evap}}_{\mathrm{CLTR}} + N^{\mathrm{Drift}}_{\mathrm{CLTR}} - N^{\mathrm{S}}_{\mathrm{CLTR},\mathrm{OUT_V},\mathrm{H_2O}} = 0 \tag{A67}$$

Set Known Cooling Tower Output Solid Concentrations.

$$x^{\mathrm{Kn}}_{\mathrm{CLTR},\mathrm{SP_{CLTR}},s} \cdot N^{\mathrm{T}}_{\mathrm{CLTR},\mathrm{SP_{CLTR}}} - N^{\mathrm{S}}_{\mathrm{CLTR},\mathrm{SP_{CLTR}},s} = 0 \quad \forall s \in S_{\mathrm{Sol}} \tag{A68}$$

Steam cycle

Set Known Process Steam Boiler Output Solid Concentrations.

$$x^{\mathrm{Kn}}_{\mathrm{X_{PWB}},\mathrm{MX_{BLR}},s} \cdot N^{\mathrm{T}}_{\mathrm{X_{PWB}},\mathrm{MX_{BLR}}} - N^{\mathrm{S}}_{\mathrm{X_{PWB}},\mathrm{MX_{BLR}},s} = 0 \quad \forall s \in S_{\mathrm{Sol}} \tag{A69}$$

Set Known Heat Engine Boiler Output Solid Concentrations.

$$x^{\mathrm{Kn}}_{\mathrm{HEP},\mathrm{MX_{BLR}},s} \cdot N^{\mathrm{T}}_{\mathrm{HEP},\mathrm{MX_{BLR}}} - N^{\mathrm{S}}_{\mathrm{HEP},\mathrm{MX_{BLR}},s} = 0 \quad \forall s \in S_{\mathrm{Sol}} \tag{A70}$$

Outlet wastewater

Upper Bound on Output Wastewater Concentrations.

$$N^{\mathrm{S}}_{\mathrm{MX_{WW}},\mathrm{OUT_V},s} - x^{\mathrm{Max}}_{\mathrm{MX_{WW}},\mathrm{OUT_V},s} \cdot N^{\mathrm{T}}_{\mathrm{MX_{WW}},\mathrm{OUT_V}} \le 0 \quad \forall s \in S_{\mathrm{WW}} \tag{A71}$$

Hydrogen/Oxygen Production

Pressure-swing adsorption

Set Recovery Fraction of H_2 from Inlet.

$$N^{\mathrm{S}}_{\mathrm{PSA},\mathrm{SP_{H_2P,H_2}}} - \mathrm{Rev}^{\mathrm{H_2}}_{\mathrm{PSA}} \cdot \sum_{(u,\mathrm{PSA})\in \mathrm{UC}} N^{\mathrm{S}}_{u,\mathrm{PSA},\mathrm{H_2}} = 0 \tag{A72}$$

Set Inlet Mole Fraction of H_2.

$$\sum_{(u,\mathrm{PSA})\in \mathrm{UC}} N^{\mathrm{S}}_{u,\mathrm{PSA},\mathrm{H_2}} - \mathrm{In}^{\mathrm{H_2}}_{\mathrm{PSA}} \cdot \sum_{(u,\mathrm{PSA})\in \mathrm{UC}} N^{\mathrm{T}}_{u,\mathrm{PSA}} = 0 \tag{A73}$$

Air separation unit

Recovery Fraction of O_2.

$$N^{\mathrm{S}}_{\mathrm{ASU},\mathrm{OUT_V},s} - (1 - \mathrm{sf}_{\mathrm{ASU}}) \cdot N^{\mathrm{S}}_{\mathrm{AC},\mathrm{ASU},s} = 0 \quad \forall s \in S^{\mathrm{U}}_{\mathrm{ASU}} \tag{A74}$$

Process Hot/Cold/Power Utility Requirements

Set Electricity Needed for Process Units.

$$Q^{\mathrm{El}}_P - \sum_{u\in U_{\mathrm{Util}}} S_u \cdot \mathrm{El}^{\mathrm{Base}}_u = 0 \tag{A75}$$

Set Cooling Water Needed for Process Units.

$$Q_P^{\mathrm{CW}} - \sum_{u \in U_{\mathrm{Util}}} S_u \cdot CW_u^{\mathrm{Base}} = 0 \tag{A76}$$

Set Heating Fuel Needed for Process Units.

$$Q_{\mathrm{FCM}} - \sum_{u \in U_{\mathrm{Util}}} S_u \cdot F_u^{\mathrm{Base}} = 0 \tag{A77}$$

Set Utilities Needed for Process Units.

$$Q_{u,ut}^{\mathrm{HU}} - S_u \cdot U_{u,ut}^{\mathrm{Base}} = 0 \qquad \forall ut, u \in U_{\mathrm{Util}} \tag{A78}$$

Process Costs

Feedstock costs

Levelized Cost of Biomass Feedstock.

$$\mathrm{Cost}_s^{\mathrm{F}} = \frac{\mathrm{MW}_s \cdot N_{\mathrm{IN_{BIO}},\mathrm{BDR},s}^{\mathrm{S}} \cdot C_s^{\mathrm{F}}}{\mathrm{Prod} \cdot \mathrm{LHV}_{\mathrm{Prod}}} \qquad \forall s \in S_{\mathrm{Bio}} \tag{A79}$$

Levelized Cost of Coal Feedstock.

$$\mathrm{Cost}_s^{\mathrm{F}} = \frac{\mathrm{MW}_s \cdot N_{\mathrm{IN_{COAL}},\mathrm{CDR},s}^{\mathrm{S}} \cdot C_s^{\mathrm{F}}}{\mathrm{Prod} \cdot \mathrm{LHV}_{\mathrm{Prod}}} \qquad \forall s \in S_{\mathrm{Coal}} \tag{A80}$$

Levelized Cost of Natural Gas Feedstock.

$$\mathrm{Cost}_s^{\mathrm{F}} = \sum_{(\mathrm{IN_{NG}},u) \in \mathrm{UC}} \frac{\mathrm{MW}_s \cdot N_{\mathrm{IN_{NG}},u,s}^{\mathrm{S}} \cdot C_s^{\mathrm{F}}}{\mathrm{Prod} \cdot \mathrm{LHV}_{\mathrm{Prod}}} \qquad \forall s \in S_{\mathrm{NG}} \tag{A81}$$

Levelized Cost of Freshwater Feedstock.

$$\mathrm{Cost}_{\mathrm{H_2O}}^{\mathrm{F}} = \frac{\mathrm{MW}_{\mathrm{H_2O}} \cdot N_{\mathrm{IN_{H_2O,SP_{WRI},H_2O}}}^{\mathrm{S}} \cdot C_{\mathrm{H_2O}}^{\mathrm{F}}}{\mathrm{Prod} \cdot \mathrm{LHV}_{\mathrm{Prod}}} \tag{A82}$$

Electricity costs

Levelized Cost of Electricity.

$$\mathrm{Cost}^{\mathrm{El}} = \frac{F_{\mathrm{In}}^{\mathrm{El}} \cdot C_{\mathrm{In}}^{\mathrm{El}} - F_{\mathrm{Out}}^{\mathrm{El}} \cdot C_{\mathrm{Out}}^{\mathrm{El}}}{\mathrm{Prod} \cdot \mathrm{LHV}_{\mathrm{Prod}}} \tag{A83}$$

CO_2 sequestration costs

Levelized Cost of CO_2 Sequestration.

$$\mathrm{Cost}^{\mathrm{Seq}} = \frac{\mathrm{MW}_{\mathrm{CO_2}} \cdot N_{\mathrm{CO_2SC,OUT_{CO_2},CO_2}}^{\mathrm{S}} \cdot C^{\mathrm{Seq}}}{\mathrm{Prod} \cdot \mathrm{LHV}_{\mathrm{Prod}}} \tag{A84}$$

Levelized investment costs

Total Overnight Cost of Process Units.

$$\mathrm{TOC}_u = (1 + \mathrm{IC}_u) \cdot (1 + \mathrm{BOP}_u) \cdot C_{o,u} \cdot \left(\frac{S_u}{S_{o,u}}\right)^{\mathrm{sf}_u} \tag{A85}$$

Variable Capital Costs of Process Units.

$$\mathrm{CC}_u = \mathrm{LCCR} \cdot \mathrm{IDCF} \cdot \mathrm{TOC}_u \tag{A86}$$

Levelized Cost of Process Units.

$$\mathrm{Cost}_u^U = \frac{\mathrm{CC}_u \cdot (1 + \mathrm{OM})}{\mathrm{CAP} \cdot \mathrm{Prod} \cdot \mathrm{LHV}_{\mathrm{Prod}}} \tag{A87}$$

Objective Function

Levelized Cost of Fuel Production.

$$\mathrm{MIN} \sum_{u \in U_{\mathrm{In}}} \sum_{(u,s) \in S^U} \mathrm{Cost}_s^{\mathrm{F}} + \mathrm{Cost}^{\mathrm{El}} + \mathrm{Cost}^{\mathrm{Seq}} + \sum_{u \in U_{\mathrm{Inv}}} \mathrm{Cost}_u^U \tag{A88}$$

Simultaneous Heat and Power Integration

Pinch points

Set Pinch Points Based on Inlet Temperatures.

$$\left\{ \begin{array}{c} T_{\mathrm{pi}} = T_{u,u'}^{\mathrm{HP\text{-}in}} \; \forall \; (u,u') \in \mathrm{HP}; T_{\mathrm{pi}} = T_u \; \forall \; u \in \mathrm{HP}t^{\mathrm{HB}}; \\ T_{\mathrm{pi}} = T_{ut} \; \forall \; (ut,\mathrm{pi}) \in \mathrm{HP}t - \mathrm{PI}^{Ut}; \; T_{\mathrm{pi}} = T_{b,c,t}^{\mathrm{PC\text{-}in}} \; \forall \; (b,c,t) \in \mathrm{HEP}; T_{\mathrm{pi}} = T_c \\ T_{\mathrm{pi}} = T_{u,u'}^{\mathrm{CP\text{-}in}} + \Delta T \; \forall \; (u,u') \in \mathrm{CP}; T_{\mathrm{pi}} = T_{b,c}^{\mathrm{EC\text{-}in}} + \Delta T \; \forall \; (b,c) \in \mathrm{CP}^{\mathrm{EC}}; \\ T_{\mathrm{pi}} = T_{b,t}^{\mathrm{SH\text{-}in}} + \Delta T \; \forall \; (b,t) \in \mathrm{CP}^{\mathrm{SH}}; T_{\mathrm{pi}} = T_{ut} + \Delta T \; \forall \; (ut,\mathrm{pi}) \in \mathrm{CP}t - \mathrm{PI}^{Ut}; \\ T_{\mathrm{pi}} = T_b + \Delta T \end{array} \right\} \tag{A89}$$

Temperature differences

Process Unit Hot Stream Inlets.

$$\Delta T_{u,u',pi}^{\mathrm{HP\text{-}in}} = \max\{0, T_{u,u'}^{\mathrm{HP\text{-}in}} - T_{\mathrm{pi}}\} \tag{A90}$$

Process Unit Hot Stream Outlets.

$$\Delta T_{u,u',\mathrm{pi}}^{\mathrm{HP\text{-}out}} = \max\{0, T_{u,u'}^{\mathrm{HP\text{-}out}} - T_{\mathrm{pi}}\} \tag{A91}$$

Process Unit Cold Stream Inlets.

$$\Delta T_{u,u',\mathrm{pi}}^{\mathrm{CP\text{-}in}} = \max\{0, T_{u,u'}^{\mathrm{CP\text{-}in}} - (T_{\mathrm{pi}} - \Delta T)\} \tag{A92}$$

Process Unit Cold Stream Outlets.

$$\Delta T_{u,u',\mathrm{pi}}^{\mathrm{CP\text{-}out}} = \max\{0, T_{u,u'}^{\mathrm{CP\text{-}out}} - (T_{\mathrm{pi}} - \Delta T)\} \tag{A93}$$

Heat Engine Precooler Inlets.

$$\Delta T_{b,c,t,\mathrm{pi}}^{\mathrm{PC\text{-}in}} = \max\{0, T_{b,c,t}^{\mathrm{PC\text{-}in}} - T_{\mathrm{pi}}\} \tag{A94}$$

Heat Engine Precooler Outlets.

$$\Delta T_{b,c,t,\mathrm{pi}}^{\mathrm{PC\text{-}out}} = \max\{0, T_{b,c,t}^{\mathrm{PC\text{-}out}} - T_{\mathrm{pi}}\} \tag{A95}$$

Heat Engine Economizer Inlets.

$$\Delta T^{\text{EC-in}}_{b,c,\text{pi}} = \max\{0, T^{\text{EC-in}}_{b,c} - (T_{\text{pi}} - \Delta T)\} \tag{A96}$$

Heat Engine Economizer Outlets.

$$\Delta T^{\text{EC-out}}_{b,c,\text{pi}} = \max\{0, T^{\text{EC-out}}_{b,c} - (T_{\text{pi}} - \Delta T)\} \tag{A97}$$

Heat Engine Superheater Inlets.

$$\Delta T^{\text{SH-in}}_{b,t,\text{pi}} = \max\{0, T^{\text{SH-in}}_{b,t} - (T_{\text{pi}} - \Delta T)\} \tag{A98}$$

Heat Engine Superheater Outlets.

$$\Delta T^{\text{SH-out}}_{b,t,\text{pi}} = \max\{0, T^{\text{SH-out}}_{b,t} - (T_{\text{pi}} - \Delta T)\} \tag{A99}$$

Heat engine logical existence

Bound on Heat Engine Flow Rate.

$$F^{\text{Up}}_{b,c,t} \cdot y^{\text{En}}_{b,c,t} \geqslant F^{\text{En}}_{b,c,t} \forall (b,c,t) \in \text{HEP} \tag{A100}$$

Bound on Total Amount of Heat Engines.

$$\sum_{(b,c,t)\in\text{HEP}} y^{\text{En}}_{b,c,t} \leq \text{EnMax} \tag{A101}$$

Heat balances

Heat Engine Electricity Balance.

$$\sum_{(b,c,t)\in\text{HEP}} (w^{\text{Tur}}_{b,c,t} - w^{\text{Pum}}_{b,c,t}) \cdot F^{\text{En}}_{b,c,t} = F_{\text{El}} \tag{A102}$$

Upper Heat Balance for Pinch Points.

$$\begin{aligned} Q^{\text{H}}_{\text{pi}} = & \sum_{(u,u')\in\text{HP}} \sum_{s} N^{s}_{u,u',s} \cdot Cp^{\text{P}}_{u,u',s} \cdot (\Delta T^{\text{HP-in}}_{u,u',\text{pi}} - \Delta T^{\text{HP-out}}_{u,u',\text{pi}}) \\ & + \sum_{(b,c,t)\in\text{HEP}} F^{\text{En}}_{b,c,t} \cdot Cp^{\text{HE-P}} \cdot (\Delta T^{\text{PC-in}}_{b,c,t,\text{pi}} - \Delta T^{\text{PC-out}}_{b,c,t,\text{pi}}) \\ & + \sum_{(ut,\text{pi})\in\text{HP}t\text{-PI}^{Ut}} \sum_{(u,ut)\in\text{HP}t} Q^{\text{HU}}_{u,ut} \\ & + \sum_{(u,\text{pi})\in\text{HP}t-\text{PI}^{\text{HB}}} Q_u + \sum_{b} \sum_{(c,\text{pi})\in\text{HP}t-\text{PI}^{\text{C}}} \sum_{t} F^{\text{En}}_{b,c,t} \cdot dH^{\text{C}}_{c} \end{aligned} \tag{A103}$$

Lower Heat Balance for Pinch Points.

$$\begin{aligned} Q^{\text{C}}_{\text{pi}} = & \sum_{(u,u')\in\text{CP}} \sum_{s} N^{s}_{u,u',s} \cdot Cp^{\text{P}}_{u,u',s} \cdot (\Delta T^{\text{CP-out}}_{u,u',\text{pi}} - \Delta T^{\text{CP-in}}_{u,u',\text{pi}}) \\ & + \sum_{(b,c,t)\in\text{HEP}} F^{\text{En}}_{b,c,t} \cdot Cp^{\text{HE-E}} \cdot (\Delta T^{\text{EC-out}}_{b,c,\text{pi}} - \Delta T^{\text{EC-in}}_{b,c,\text{pi}}) \\ & + \sum_{(b,c,t)\in\text{HEP}} F^{\text{En}}_{b,c,t} \cdot Cp^{\text{HE-S}} \cdot (\Delta T^{\text{SH-out}}_{b,t,\text{pi}} - \Delta T^{\text{SH-in}}_{b,t,\text{pi}}) \\ & + \sum_{(ut,\text{pi})\in\text{CP}t-\text{PI}^{Ut}} \sum_{(u,ut)\in\text{CP}t} Q^{\text{HU}}_{u,ut} + \sum_{(b,\text{pi})\in\text{CP}t-\text{PI}^{\text{B}}} \sum_{c} \sum_{t} F^{\text{En}}_{b,c,t} \cdot dH^{\text{B}}_{b} \end{aligned} \tag{A104}$$

Pinch Point Heating Deficit.

$$z_{\text{pi}} = Q^{\text{C}}_{\text{pi}} - Q^{\text{H}}_{\text{pi}} \tag{A105}$$

Negativity of Pinch Deficits.

$$z_{\text{pi}} \leq 0 \tag{A106}$$

Total Heating Deficit.

$$\Omega - Q_c = 0 \tag{A107}$$

Total Heat Balance.

$$\begin{aligned} \Omega = & \sum_{(u,u')\in\text{HP}} \sum_{s} N^{s}_{u,u',s} \cdot Cp^{\text{P}}_{u,u',s} \cdot (T^{\text{HP-in}}_{u,u'} - T^{\text{HP-out}}_{u,u'}) \\ & + \sum_{(b,c,t)\in\text{HEP}} F^{\text{En}}_{b,c,t} \cdot Cp^{\text{HE-P}} \cdot (T^{\text{PC-in}}_{b,c,t} - T^{\text{PC-out}}_{b,c,t}) \\ & + \sum_{(u,ut)\in\text{HP}t} Q^{\text{HU}}_{u,ut} + \sum_{u\in\text{HP}t^{\text{HB}}} Q_u + \sum_{(b,c,t)\in\text{HEP}} F^{\text{En}}_{b,c,t} \cdot dH^{\text{C}}_{c} \\ & - \sum_{(u,u')\in\text{CP}} \sum_{s} N^{s}_{u,u',s} \cdot Cp^{\text{P}}_{u,u',s} \cdot (T^{\text{CP-out}}_{u,u'} - T^{\text{CP-in}}_{u,u'}) \\ & - \sum_{(b,c,t)\in\text{HEP}} F^{\text{En}}_{b,c,t} \cdot Cp^{\text{HE-E}} \cdot (T^{\text{EC-out}}_{b,c} - T^{\text{EC-in}}_{b,c}) \\ & - \sum_{(b,c,t)\in\text{HEP}} F^{\text{En}}_{b,c,t} \cdot Cp^{\text{HE-S}} \cdot (T^{\text{SH-out}}_{b,t} - T^{\text{SH-in}}_{b,t}) \\ & - \sum_{(u,ut)\in\text{CP}t} Q^{\text{HU}}_{u,ut} - \sum_{(b,c,t)\in\text{HEP}} F^{\text{En}}_{b,c,t} \cdot dH^{\text{B}}_{b} \end{aligned} \tag{A108}$$

Manuscript received Aug. 31, 2012, and revision received Nov. 28, 2012.